JAMES | Journal of Advances in Modeling Earth Systems

RESEARCH ARTICLE
10.1029/2018MS001536

Precipitation Characteristics in the Community Atmosphere Model and Their Dependence on Model Physics and Resolution

Di Chen[1] **and Aiguo Dai**[1]

[1]Department of Atmospheric and Environmental Sciences, University at Albany, State University of New York, Albany, NY, USA

Key Points:
- Reducing convective precipitation and/or increasing resolution alleviate the *drizzling* problem in CAM
- Different cloud microphysics schemes largely contribute to precipitation differences between CAM4 and CAM5
- Resolution dependence in CAM is a combination of grid aggregation effects and physical adjustments

Correspondence to:
A. Dai,
adai@albany.edu

Citation:
Chen, D., & Dai, A. (2019). Precipitation characteristics in the Community Atmosphere Model and their dependence on model physics and resolution. *Journal of Advances in Modeling Earth Systems*, *11*, 2352–2374. https://doi.org/10.1029/2018MS001536

Received 19 OCT 2018
Accepted 3 JUL 2019
Accepted article online 10 JUL 2019
Published online 28 JUL 2019

Abstract Precipitation amount (A), frequency (F), intensity (I), and duration (D) are important properties of precipitation, but their estimates are sensitive to data resolution. This study investigates this resolution dependence, and the influences of different model physics, by analyzing simulations by the Community Atmospheric Model (CAM) version 4 (CAM4) and version 5 (CAM5) with varying grid sizes from ~0.25 to 2.0°. Results show that both CAM4 and CAM5 greatly overestimate F and D but underestimate I at all resolutions, despite realistic A. These biases partly result from too much parameterized (convective) precipitation with high F and D but low I. Different cloud microphysics schemes contribute to the precipitation differences between CAM4 and CAM5. The A, F, I, and D of convective and nonconvective precipitation react differently to grid-size decreases, leading to the large decreases in F and D but increases in the I for total precipitation as model resolution increases. This resolution dependence results from the increased probability of precipitation over a larger area (area aggregation effect, which is smaller than in observations) and the varying performance of model physics under changing resolution (model adjustment effect), which roughly enhances the aggregation-induced dependence. Finer grid sizes not only increase resolved precipitation, which has higher intensity and thus improves overall precipitation intensity in CAM, but also reduce the area aggregation effect. Thus, the long-standing *drizzling* problem in climate models may be mitigated by increasing model resolution and modifying model physics to suppress parameterized convective precipitation and enhance resolved nonconvective precipitation.

1. Introduction

To fully characterize a discontinuous variable like precipitation, one often needs not only the accumulative amount (A) but also its frequency (F, the percentage of time it precipitates), intensity (I, the precipitation rate averaged over the precipitating time only), and duration (D, mean precipitating interval averaged over all precipitation events; Dai et al., 2007; Trenberth et al., 2003, 2017). While precipitation A (or mean rate) is important and is the subject of most studies on precipitation, precipitation F and I also have large impacts on surface runoff, soil moisture, and surface heat fluxes over land (Qian et al., 2006; Trenberth, 2011). Moreover, they serve as additional metrics for evaluating physics parametrizations in numerical weather and climate models, which still show considerable biases in simulated precipitation F and I (Dai, 2006; DeMott et al., 2007).

Precipitation F ranges from close to zero over deserts to around 50% over northern high latitudes in winter (Dai, 2001), although it depends on the area and threshold used to detect precipitation. Recently, Trenberth and Zhang (2018a) analyzed hourly precipitation data on a 0.25° grid from satellite observations and showed that precipitation (defined as above 0.02 mm/hr) occurs about 11.0 ± 1.1% (±1 standard deviation or SD) of the time averaged over 60°S–60°N, but only about 8% of the time over land. Previous studies have shown that precipitation spatial variations, its diurnal, and annual cycles are largely determined by how often it rains (i.e., the F) rather than how intense it rains (i.e., the I), with the I only having about half of the diurnal amplitude seen in the F and A (Chen & Dai, 2018; Dai et al., 1999; Dai et al., 2007). Furthermore, precipitation F is dominated by light-to-moderate precipitation events (Dai et al., 2017), and it peaks in the intertropical convergence zone (ITCZ) and high-latitude winter (Chen & Dai, 2018; Dai, 2001; Trenberth & Zhang, 2018a). Pendergrass and Deser (2017) showed that the spatial distribution and seasonal cycle of the F are similar to those of total rainfall amount, yet the F peak varies inversely with the range of rain rates. Thus, precipitation F tends to play a bigger role in determining the spatial patterns, the diurnal

cycle and the seasonal variations of precipitation over most of the globe, whereas precipitation intensity has important implication for precipitation extreme and its future changes (Dai et al., 2017; Trenberth et al., 2003; Wehner et al., 2014).

Changes in precipitation I under greenhouse gas (GHG)-induced global warming is a big concern, as increased water vapor could lead to more intense storms (Dai et al., 2017; Trenberth et al., 2003). It is projected that precipitation F and I are likely to behave differently in the future, with the I expected to increase (by ~7%/K on average, mostly following water vapor increase rates) while the overall precipitation F is expected to decrease (mostly for light-to-moderate precipitation, Dai et al., 2017; Lau et al., 2013; Pendergrass & Hartmann, 2014a; Trenberth et al., 2003). Few studies have addressed precipitation D, either using observations or models. Trenberth et al. (2017) found that the D estimated using the CPC MORPHing technique (CMORPH) 3-hourly satellite product is around 12–15 hr over the tropical and subtropical oceans, but the 3-hourly satellite data from the Tropical Rainfall Measuring Mission (TRMM) produce only about 80–85% of the D values from CMORPH. Most climate models project a decrease in D over the 21st century, although the decrease is less than 1% /K in the multimodel mean (Dwyer & O'Gorman, 2017).

Current global climate models (GCMs) tend to overestimate precipitation F and D but underestimate I, even though precipitation A is realistic (e.g., Dai, 2006; DeMott et al., 2007; Flato et al., 2013; Trenberth & Zhang, 2018b). This means that the models produce realistic A from incorrect combination of F and I, that is, raining too frequently at reduced intensity (Dai, 2006). A cause of this *drizzling* bias is model's frequent firing of moist convection, whereas convective inhibition processes (e.g., large-scale subsidence) often allow atmospheric instability to accumulate before intense convection starts in the real world (Dai & Trenberth, 2004). Wilcox and Donner (2007) suggested that the simulated precipitation I is affected by several aspects of the convective parameterization, including the closure, assumed convective triggers, and the spectrum of the convective and mesoscale clouds. In the Community Earth System Model version 1 (CESM1), daily precipitation duration can exceed 20 hr over many oceanic places yet heavy rain is far from enough (Trenberth & Zhang, 2018a). Herold et al. (2016) noted that atmospheric reanalyses and CMIP5 models tend to oversimulate wet days, which is consistent with the drizzling problem found in many earlier climate models (Dai, 2006; Dai & Trenberth, 2004). Some studies (Xie et al., 2004; Zhang et al., 2003) attempted to relieve this drizzling problem in models, but a satisfactory solution is still lacking.

For global models with grid spacing of 20–100 km or more, explicit representation of organized mesoscale convective systems, easterly waves, tropical storms, and so forth is often inadequate in these models (Trenberth et al., 2017). Models with higher resolutions, such as convection-permitting simulations with grid spacing of less than 4 km (Kendon et al., 2016; Prein et al., 2015), are likely to resolve these mesoscale phenomena more realistically and produce more reasonable precipitation characteristics and their response to future warming (Dai et al., 2017). Besides these physical improvements, models with finer grid sizes should produce lower F and higher I simply because of the reduced area aggregation effect discussed in Chen and Dai (2018). Thus, the drizzling problem in coarse-resolution global models is likely to become less of an issue as the model resolution increases.

The spatial and temporal resolutions of the input data can substantially alter the estimated F and I values (Biasutti & Yuter, 2013; Chen & Dai, 2018; Gehne et al., 2016; Trenberth & Zhang, 2018a). Using satellite hourly precipitation data on a 0.25° grid over a near-global (60°N–60°S) domain, Trenberth and Zhang (2018a) found that the precipitation frequency values calculated using data averaged onto a 1° grid are 35% higher than those based on 0.25° data; and on average, the frequency estimated using 3-hourly (daily) precipitation is about 25% (150%) higher than that using hourly data. Chen and Dai (2018) systematically quantified the dependence of the estimated F and I on data resolution using 3-hourly precipitation data on a 0.25° grid from two satellite products. Besides the relationship noticed by previous studies, they further showed that the dependence of F on data resolution can be explained entirely by the increased probability of precipitation over a larger area or longer time period. Thus, large differences in the estimated F and I can arise purely from the differences in the spatial or temporal resolution of the input data. It has also been suggested that spatial resolution has an important impact on the estimated precipitation duration (Nikolopoulos et al., 2017).

Such resolution dependence of precipitation characteristics is also expected to exist in climate models with different resolutions, not only among different models but also for one model configured with

different resolutions. Bacmeister et al. (2014) found that the simulated climate using the Community Atmosphere Model (CAM) with high resolution (0.23° lat × 0.31° lon) is not dramatically improved compared with lower-resolution simulations. However, they noted that as resolution increases, nonconvective precipitation increases to around 50% of the total precipitation while convective precipitation decreases, which become closer to TRMM observational estimates (Dai, 2006), and the CAM4 surpasses CAM5 in this respect. Kooperman et al. (2018) also suggested that the intensity, geographic pattern, and climate change response of CAM5's nonconvective precipitation are more consistent with TRMM 3B42 than convective precipitation. O'Brien et al. (2013) investigated the dependence of the simulated clouds and precipitation in CAM4 and CAM5 on different horizontal resolutions and found that precipitation I increases as resolution increases, and this is closely related to cloud-size changes. This dependence of I on model resolution is expected since intense rainstorms tend to occur over a small area, and precipitation rates averaged over a large area such as a GCM grid box would be lower than those averaged only over the intense rainstorms. Furthermore, Rauscher et al. (2016) argued that fluid continuity, together with scaling properties of horizontal wind fields, leads to enhanced updraft and intensified resolvable-scale precipitation as resolution increases. Updrafts are strongly correlated with extreme precipitation (Li et al., 2011), and several studies (e.g., Kopparla et al., 2013; Wehner et al., 2014) found that CAM-simulated extreme daily precipitation amount is overall larger and more realistic in high resolution than in lower-resolution configurations. Benedict et al. (2017) investigated the sensitivities of precipitation A and F and extreme precipitation to model physics, horizontal resolution, and ocean type, using idealized CAM aqua-planet simulations. They found that precipitation A and F are most sensitive to the choice of horizontal grid spacing, whose impact on precipitation A and F also depends on the choice of model physics packages, especially for tropical precipitation A and F.

The resolution dependence reported in these previous studies can result from two different effects: the area aggregation effect, which refers to the increased probability of precipitation as the sampling (or averaging) area increases (Chen & Dai, 2018); and the effect of model adjustments to varying resolutions, which refers to the different performance of model physics and model dynamics under changing model resolutions. For example, finer model resolutions can increase the resolved (mostly large-scale) precipitation but reduce parameterized (mostly convective) precipitation (Bacmeister et al., 2014; Kooperman et al., 2016, 2018; O'Brien et al., 2013, 2016). Finer resolutions can also resolve terrain and orographic features better, leading to improved precipitation simulations. As shown below, the F, I, and D values differ substantially in CAM for the resolved and parameterized precipitation, and therefore, a change in their partitioning can affect the characteristics of the total precipitation.

While the recent studies mentioned above have improved our knowledge about model-simulated precipitation, many issues still remain. For example, what are the differences in the F, I, and D for the resolved (referred to as nonconvective in CAM) and parameterized (referred to as convective in CAM) precipitation, and how can these differences affect the characteristics of the total precipitation? It is also unclear to what extent the resolution dependence of the simulated precipitation characteristics results from the pure area aggregation effect and from the model adjustment effect. Answers to these questions can improve our understanding of the dependence of the precipitation characteristics on data resolution, and they may also help diagnose the origins of model precipitation biases and provide guidance for future model improvements. To address these issues, we performed and analyzed a series of carefully designed simulations with varying resolutions using the CAM4 and CAM5. Our focus is on what causes the resolution dependence of the A, F, I, and D in CAM and how the resolved and parameterized precipitation differs in these characteristics. New aspects of our study include (1) an attribution of the resolution dependence of the F, I, and D to the area aggregation and model adjustments to different resolutions; (2) an analysis of the different precipitation F, I, and D between convective and nonconvective precipitation in CAM and how that affects the overall characteristics of precipitation as the model resolution changes; and (3) a diagnostic analysis of the impact of different cloud microphysics schemes in CAM4 and CAM5 on the simulated precipitation characteristics.

The paper is organized as follows. Section 2 describes the model setups and simulations, and the observational data sets. Section 3 presents the main results of simulated precipitation characteristics and their dependence to spatial resolutions. Section 4 summarizes the key findings and discusses some caveats and future work.

2. Data and Method

2.1. Model Description and Experiments Design

To understand precipitation characteristics in climate models and their dependence on data resolution, we utilized CESM version 1.2.1 (Hurrell et al., 2013) with CAM4 (Neale et al., 2010) and CAM5 (Neale et al., 2012) for two groups of experiments, both comprise 3–4 simulations, which differ only in horizontal resolution. Group A uses the component set *F_2000*, which consists of CAM4, Community Land Model (CLM) 4.0, prescribed Community Ice CodE (CICE4) and present-day climatological data ocean model. This component set makes the simulations relatively simple as the ocean (i.e., sea surface temperatures) and sea ice are prescribed using present-day monthly climatology (for 1982–2011) from Hadley Centre Sea Ice and Sea Surface Temperature (HadISST) data set (Neale et al., 2012). Group A simulations using CAM4 were configured on four different horizontal grids including 0.23° lat × 0.31° lon, 0.47° × 0.63°, 0.9° × 1.25° and 1.9° × 2.5°(abbreviated as 0.25, 0.5, 1.0, and 2.0°, respectively). Group B simulations were similar to Group A except CAM5 was used. Group B consists of simulations on 0.5, 1.0, and 2.0° grids, as a test run with 0.25° gird turned out to be too computationally expensive for us to carry out due to the more sophisticated treatment of aerosol-cloud interactions in CAM5 (Neale et al., 2012). Finite volume dynamical core was employed in both groups. The time step length for the simulations is similar to Wehner et al. (2014), that is, 900 s for 0.25° grid and 1,800 s for 0.5, 1.0 and 2.0° grids for the model physics. Williamson (2013) showed that a change in the physical time step may affect the performance of the Zhang and McFarlane (1995) deep convection scheme and therefore may change the partitioning between the stratiform and convective precipitation in CAM. This may affect our results on the 0.25° grid in comparison with the other grids. We did not perform any tuning of the model as the resolution changes. Bacmeister et al. (2014) showed that the top-of-atmosphere energy balance is similar with and without tuning for CAM4 simulations on 0.25° grid.

All simulations were run for five model years, and hourly outputs were saved for analysis. Since we used the monthly SST (and sea ice) climatology to force the models, which were initialized using realistic fields from a prior simulation (and therefore the models did not need to be spun up), the precipitation statistics (for A, F, I, and D) calculated from the hourly data from the 5-year simulations should be stable and representative of their climatology, especially for their zonal mean values. Since all the simulations were started from the same initial conditions and forced by the same climatological ocean conditions, the effects of atmospheric internal variability on the 5-year mean precipitation are likely to be small, which is confirmed by the small differences in precipitation amount among the different simulations. This allows us to attribute most of the differences of the estimated precipitation statistics among the simulations to changes in model resolution or model physics. Also, we focus on the annual mean results, since the seasonal results on the resolution dependence do not differ greatly. The details of the experiment configurations are listed in Table 1.

Substantial differences exist between CAM4 and CAM5 physics (Table 2), including but not limited to (1) turbulence scheme: CAM4 uses a dry turbulence scheme (Holtslag & Boville, 1993), while CAM5 uses a moist turbulence scheme based on a diagnostic turbulent kinetic energy formulation and a first-order K-diffusion scheme with entrainment (Bretherton & Park, 2009); (2) shallow convection scheme: CAM4 uses Hack (1994) scheme, while CAM5 uses one that is specifically designed to interact with the new moist turbulence scheme in order to prevent double counting seen in previous CAM parameterizations (Park & Bretherton, 2009); (3) cloud microphysics parameterization: CAM4 uses prognostic *RK* single-moment scheme (Rasch & Kristjánsson, 1998) while CAM5 uses prognostic *MG* double-moment scheme (Morrison & Gettelman, 2008; Gettelman et al., 2008, see more details below); and (4) radiation scheme: CAM4 uses the radiation scheme developed for CAM by Collins et al. (2004) while CAM5 uses the Rapid Radiative Transfer Method for GCMs (RRTMG, Neale et al., 2012). The same deep convection parameterization (Zhang & McFarlane, 1995) is used in CAM4 and CAM5. Most previous studies using CAM4 and CAM5 utilized the highly idealized aqua-planet configuration (Benedict et al., 2017; O'Brien et al., 2013, 2016; Zarzycki et al., 2014), rather than the realistic land-ocean configuration used here.

2.2. Observational Data Sets

Observational precipitation data sets from TRMM and the Global Precipitation Climatology Project (GPCP) were used to evaluate model simulations. Details of these data sets are listed in Table 3. The main data set is the blended 3-hourly precipitation data on a 0.25° grid from TRMM 3B42 (Huffman et al., 2007; TRMM 3B42 documentation, 2011b). The TRMM 3B42 forcefully adjusted the satellite estimates up to the magnitude

Table 1
CAM Simulations Configurations

Experiment group	Simulation number	Components set	Grid configurations	Time step lengths (dtime)
A (CAM4)	A1	F_2000	0.23 × 0.31_gx1v6 (f02_g16)	900 s
	A2	Components: CAM4, CLM4.0, DOCN, and CICE	0.47 × 0.63_gx1v6 (f05_g16)	
	A3	Description: CAM4 physics forced	0.9 × 1.25_gx1v6 (f09_g16)	
	A4	by climatological SSTs and sea ice	1.9 × 2.5_gx1v6 (f19_g16)	1,800 s
B	B1	F_2000_CAM5	0.47 × 0.63_gx1v6 (f05_g16)	
(CAM5)	B2	Components: CAM5, CLM4.0, DCON, and CICE	0.9 × 1.25_gx1v6 (f09_g16)	
	B3	Description: CAM5 physics forced by climatological SSTs and sea ice	1.9 × 2.5_gx1v6 (f19_g16)	

Note. CAM4 = Community Atmospheric Model version 4; CAM5 = Community Atmospheric Model version 5; CLM4.0 = Community Land Model 4.0; DOCN = climatological data ocean model; CICE = Community Ice CodE.

indicated by monthly gauge analysis from GPCP (Huffman et al., 2007). Dai et al. (2007) showed that spatial patterns in the mean precipitation amount from the TRMM 3B42 are comparable to other monthly products like GPCP v2.2 (Huffman et al., 2009). The advantage of TRMM 3B42 is its high spatial and temporal resolution, which better serves the purpose of studying precipitation characteristics including F, I, and D. The TRMM 3A25 product determines rain types by a vertical profile method (V-method) and a horizontal pattern method (H-method, Awaka et al., 1997, 2007; Yang & Smith, 2008). Both methods classify rain into three categories: stratiform, convective, and other (a small part, TRMM 3A25 documentation, 2011a). We used this product to validate the simulated convective-to-total precipitation ratio with the recognition that the definition of convective versus stratiform in TRMM observations is not identical to the definition of convective versus nonconvective precipitation in GCMs as noticed previously (Dai, 2006; Held et al., 2007; Pendergrass & Hartmann, 2014a). That is, we used the range of TRMM partitioning ratios as an approximate reference and model partitioning ratios greatly outside this range would be considered biased. We also used GPCP v2.2 monthly precipitation data to evaluate the model-simulated precipitation amount.

To improve the comparability, model outputs and observational data sets were remapped (by averaging without spatial interpolation) onto similar spatial and temporal resolutions. For instance, to be consistent with the groups A and B simulations on the 0.5° grid, the original TRMM 3B42 data on a 0.25° grid were simply averaged onto a 0.5° lat × 0.5° lon grid, which is close to the 0.5° model grid of 0.47° lat × 0.63° lon, before calculating F, I, and D. The hourly model output was also aggregated into 3-hourly precipitation rates for comparison with the TRMM 3B42 data. Likewise, to be consistent with the GPCP data, CAM4 and CAM5 outputs on the 0.5° grid were averaged onto the 2.5° grid of the GPCP for comparison between them, although precipitation amount is insensitive to spatial and temporal resolution (Chen & Dai, 2018). Additionally, we used the same threshold of $P > 0.1$ mm/hr for nondrizzle 3-hourly (and also for the hourly model) precipitation as in Dai et al. (2007) for calculating F, I, and D, noting that the F, I, and D are sensitive to this threshold (Chen & Dai, 2018; Zhou et al., 2008). The calculation of the F and I follows Chen and Dai (2018). The duration is the length of a continuous precipitation event during which all the hourly (or 3-hourly) precipitation rates exceed the 0.1 mm/hr threshold, and it is averaged over all the precipitation events to derive the mean D shown below.

Table 2
Major Physics Schemes in CAM4 and CAM5

Physics schemes	CAM4	CAM5
Turbulence scheme	Dry turbulence scheme	Moist turbulence scheme
Shallow convection scheme	Hack scheme	Park and Bretherton scheme
Deep convection scheme	Zhang and McFarlane scheme	
Cloud microphysics parameterization	Prognostic single-moment scheme	Prognostic double-moment scheme
Radiation scheme	CAM-RT	RRTMG

Note. CAM4 = Community Atmospheric Model version 4; CAM5 = Community Atmospheric Model version 5; RRTMG = Rapid Radiative Transfer Method for global climate models.

Table 3
Precipitation Data Sets Used in this Study and Their Sources

Data Set	Resolution and coverage	Data sources and merging method	Online documentation
TRMM 3B42	0.25° grid, 50°S-50°N, 180°W–180°E; 3-hourly precipitation rates, January 1998 to December 2014	Microwave (TRMM, SSM/I, AMSR, and AMSU) precipitation estimates were used to adjust IR estimates from geostationary IR observations. The rainfall estimates were scaled to match the monthly rain-gauge analysis used in TRMM 3B-43	https://pmm.nasa.gov/data-access/downloads/trmm
TRMM 3A25	0.5° grid, 37°S–37°N, 180°W–180°E; monthly rates for stratiform and convective precipitation, January 1998 to December 2014	PR Rainfall computes monthly statistics of the level-2 PR (V-method and H-method) measurements at both a low horizontal resolution (5° × 5°) and a high horizontal resolution (0.5° × 0.5°). For the high-resolution grids in the planetary grid 2 structure, mean rain rate along with standard deviation and rain fractions are computed.	https://pmm.nasa.gov/data-access/downloads/trmm
GPCP v2.2	2.5° grid, globe, monthly precipitation, January 1998 to December 2014	IR estimates were calibrated by microwave estimates and then adjusted by rain-gauge data	http://precip.gsfc.nasa.gov/

Note. GPCP = Global Precipitation Climatology Project; TRMM = Tropical Rainfall Measuring Mission; SSM/I = Special Sensor Microwave Imager; AMSR = Advanced Microwave Scanning Radiometer; AMSU = Advanced Microwave Sounding Unit.

3. Results

3.1. Precipitation Characteristics in CAM4 and CAM5

3.1.1. Precipitation Amount

Like most GCMs, our CAM simulations reproduce the broad patterns of the mean precipitation amount seen in GPCP data (Figure 1). Precipitation features over the ITCZ, the midlatitudes, and the dry areas (over North Africa, eastern Pacific, and Atlantic) are well simulated. However, the ITCZ in CAM4 (Figure 1a) and CAM5 (Figure 1b) are about 2–4 mm/day wetter than GPCP, especially in CAM5, although GPCP is slightly drier than another satellite product in these areas (Dai, 2006). Both models show the unrealistic *double ITCZ* over the central and eastern Pacific and the Indian Ocean, a long-standing deficiency seen in other models (Dai, 2006), while Eurasia is drier than observations. Our analyses also revealed that CAM can reproduce the broad seasonal variations of major monsoon systems, including the Indian, East Asia, and West Africa monsoons (figures not shown).

As seen in many other models (Bacmeister et al., 2014; Dai, 2006), CAM also produces too much convective precipitation at low latitudes compared with TRMM 3A25 (Figure 2c), although the definitions of rain types are not identical. TRMM 3A25 classifies precipitation types using the bright band and the shape of radar reflectivity, while CAM produces convective precipitation through its convective parameterization schemes and nonconvective precipitation through its cloud microphysics scheme (O'Brien et al., 2016). Further, the TRMM estimates of the convective versus stratiform precipitation ratio may contain uncertainties. While there are inconsistencies between model and observation in the definition of the convective versus stratiform precipitation, we use TRMM estimates as a reference point instead of absolute values. Nevertheless, a convective versus total precipitation ratio exceeding 80% (as in CAM5) is very likely to be too high, as also noted by previous studies (Bacmeister et al., 2014; Dai, 2006; Rasch et al., 2006; Yang & Smith, 2008). The convective precipitation becomes even more excessive in CAM5 than in CAM4, while nonconvective precipitation is comparable outside the low latitudes but is less in CAM5 than in CAM4 at low latitudes (Figure 2). Given that total precipitation (Figure 1) is comparable in the two models, the different partitioning of the convective and nonconvective precipitation indicates large effects of the new cloud microphysics scheme used in CAM5, since the same Zhang and McFarlane (1995) deep convection scheme, which produces most of the convective precipitation in CAM, was used in both models (Table 2).

3.1.2. Precipitation Frequency, Intensity, and Duration

Figure 3 shows precipitation F, I, and D estimated using 3-hourly total precipitation from CAM4 and CAM5 with the 0.5° model resolution and from TRMM 3B42 (averaged onto a 0.5° grid). It is clear that CAM considerably overestimates F and D while underestimates I (note the I in Figure 3f is multiplied by 0.5 for using the same color scale). Over the ITCZ, the F in the models (60–70%) is 2–3 times as that in TRMM (20–30%)

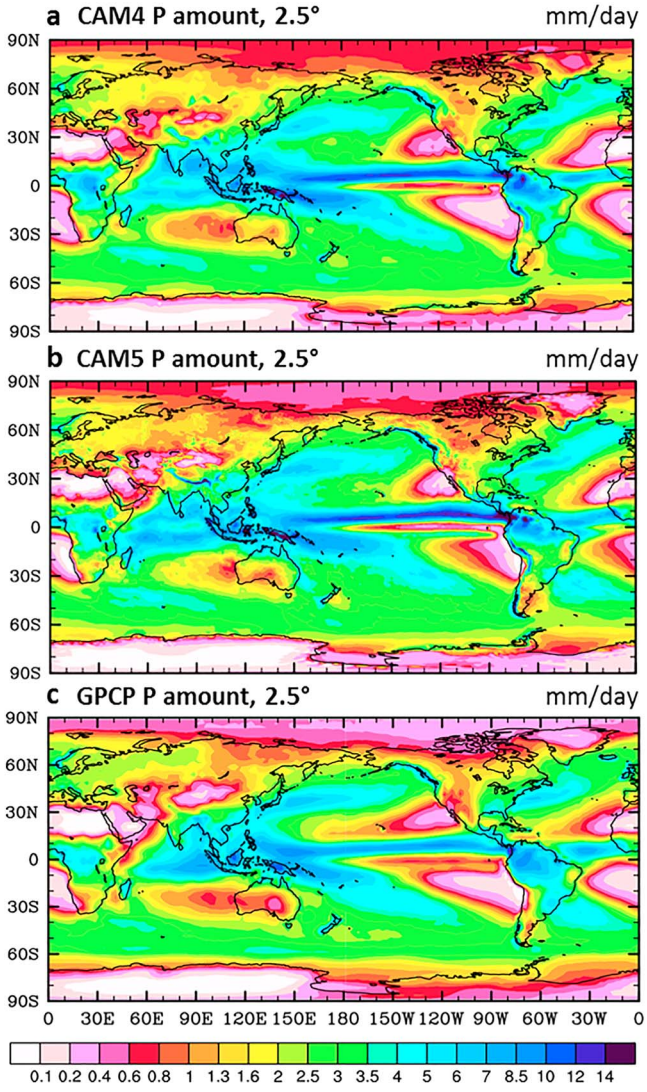

Figure 1. Mean annual precipitation amount (A, in mm/day) estimated from simulations using (a) CAM4 and (b) CAM5 (originally on 0.47° lat × 0.63° lon resolution, averaged to 2.5° lat × 2.5° lon resolution, same as GPCP). (c) The 1998–2014 mean precipitation from GPCP v2.2. CAM4 = Community Atmospheric Model version 4; CAM5 = Community Atmospheric Model version 5; GPCP = Global Precipitation Climatology Project.

and the D has a similar bias there (5–9 hr from TRMM vs 18–20 hr from both models). Overall, CAM4 and CAM5 substantially underestimate the I compared with TRMM (Figure 3f). The results are consistent with the known F and I biases in GCMs (e.g., Dai, 2006; Flato et al., 2013). The enduring problem of GCMs raining too frequently at reduced intensity (Dai, 2006) has yet been solved.

For total precipitation (i.e., convective plus nonconvective), zonal mean F is much higher while the I is substantially lower in CAM than for TRMM, although the broad shape of zonal distributions is captured (Figures 4a and 4d). The frequency peak over the ITCZ is 20% in TRMM while it is 50% in CAM4 and 54% in CAM5, and the intensity peaks over the ITCZ at 1.3 mm/hr in TRMM but less than 0.6 mm/hr in CAM. Over the tropics, the frequency for total precipitation is higher in CAM5 than in CAM4 due to the higher frequency of convective precipitation in CAM5 (Figure 4b), while nonconvective precipitation is up to 10% more frequent in CAM4 than CAM5 over most latitudes (Figure 4c). Convective precipitation events dominate in the tropics; nonconvective events are more frequent over the extratropics (Figures 4b and 4c). Precipitation intensity is stronger for nonconvective events than for convective events over the middle-low latitudes (Figures 4e and 4f). CAM5 likely excels CAM4 in this respect, as observational studies suggest global stratiform precipitation (predominantly over the ocean) intensity is higher than convective precipitation intensity (Houze et al., 2015; Schumacher & Houze, 2003; Yang & Smith, 2008). Consistent with the high frequency, mean duration (D) of all precipitation events is much longer in the two models than in TRMM, particularly over the tropics and subtropics (Figure 4g). Precipitation events last longer in CAM5 than in CAM4 (Figure 4g), contributing to CAM5's higher frequency (Figure 4a). Convective precipitation D largely resembles that of total precipitation over the tropics and subtropics (Figures 4g and 4h), and it contributes greatly to the frequency of convective precipitation (Figure 4b).

The long D (above 10 hr) for convective precipitation events really suggests that moist convection is very unrealistic in the models, since such events rarely last more than a few hours at a given location in the real world. This apparent bias in D (and F) can partly result from the fact that any convection event over a fraction of a GCM grid box may produce enough precipitation so that the grid-mean rain rate would exceed the minimum threshold of a precipitation event and therefore all such convective events over any parts of the GCM grid box would lead to a grid-box-wide precipitation event. For example, if a moist convection occurs in the 01Z, 02Z, 03Z, and 04Z hour, respectively, over only the upper-left, upper-right, lower-left, and lower-right corners of a GCM grid box, then the duration of these individual events is just 1 hr, but the duration of the convective precipitation based on the GCM grid-box-mean precipitation rate would be 4 hr. This illustrates the area aggregation effect (as discussed in Chen & Dai, 2018) using data averaging over a large area within one GCM grid box. More discussions on the area aggregation effect across different model resolutions can be found in section 3.2.3.

3.1.3. CAM4 and CAM5 Precipitation Differences Due to Microphysics Schemes

Given the large differences in the partitioning of the convective (from the convection scheme) and nonconvective (from the cloud microphysics scheme) precipitation between CAM4 and CAM5, it is reasonable to speculate that the different cloud microphysics schemes of CAM4 and CAM5 may have played a big role. The major difference between the two microphysics schemes is the treatment of the number concentration in the cloud and precipitation particle size distribution functions. The Rasch and Kristjánsson (1998, hereafter RK98) one-moment (1 M) scheme in CAM4 does not track the number concentration but specify a

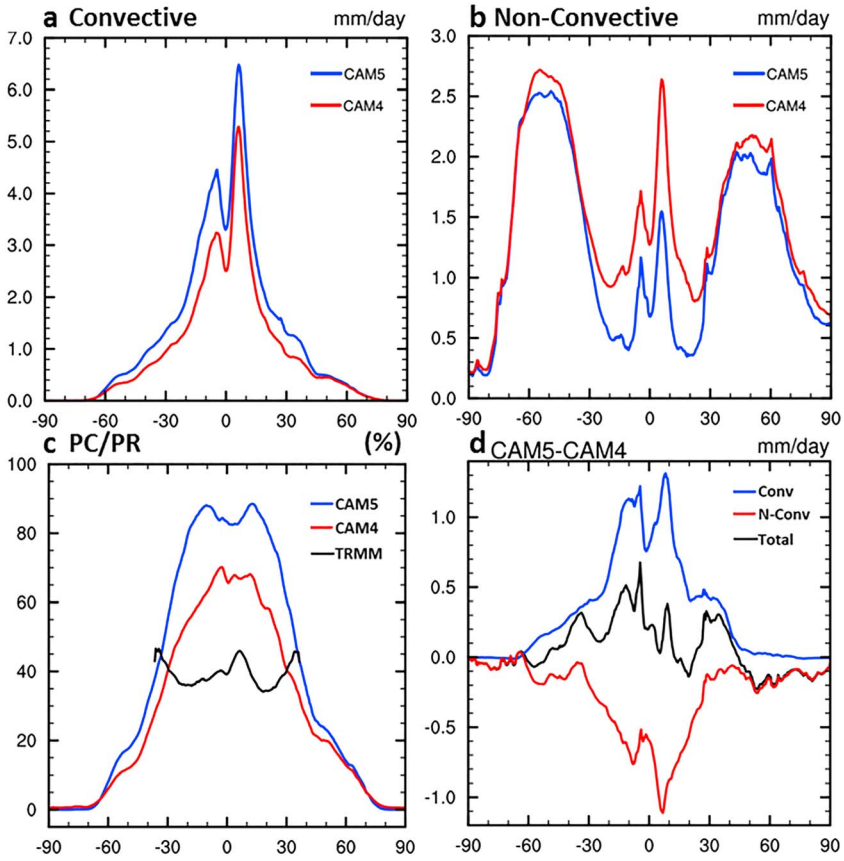

Figure 2. Zonal mean annual (a) parameterized convective precipitation, (b) resolved nonconvective precipitation, (c) convective-to-total (PC/PR) precipitation ratio, and (d) the CAM5-minus-CAM4 difference of total, convective, and nonconvective precipitation amount. Results are calculated based on outputs from CAM4 and CAM5 simulations on 0.47° lat × 0.63° lon resolution. The black line in Figure 2c is the convective-to-total precipitation ratio from TRMM 3A25 data of 1998–2014 on a 0.5° grid. CAM4 = Community Atmospheric Model version 4; CAM5 = Community Atmospheric Model version 5; TRMM = Tropical Rainfall Measuring Mission.

fixed intercept parameter N_0, while the Morrison and Gettelman (2008, hereafter MG08) two-moment (2 M) scheme in CAM5 updates N_0 using the predicted number concentration N (Gettelman et al., 2008; Morrison & Gettelman, 2008).

Gettelman et al. (2008) compared the cloud characteristics simulated by the MG08 and RK98 schemes, both are implemented in version 3 of CAM (CAM3) physics with other components unchanged. They found that the MG08 scheme produces smaller particle sizes than the RK98 scheme. As similar sensitivity tests (i.e., substituting the RK98 scheme with the MG08 scheme in CAM4, or vice versa in CAM5) are not straightforwardly available for us to carry out, we reproduced Figure 5 of Gettelman et al. (2008) using our simulation output. Overall, the probability density function (Figure 5) are similar to their CAM3-based results. Cloud droplet effective radius (Figure 5a) peaks at 9–11 μm, similar to Gettelman et al. (2008), whereas the RK98 scheme specifies droplet sizes that are mostly 14 μm over both land and ocean (Collins et al., 2004). The droplet number concentration (Figure 5c) peaks around 30–80 cm^{-3} over land and ocean; the values are smaller than specified in RK98 scheme (400 cm^{-3} over land and 150 cm^{-3} over ocean; Neale et al., 2010). The effective radius of ice particles (Figure 5b) agrees with the specified values of 20–30 μm in the RK98 scheme, while the number concentration is smaller than Gettelman et al. (2008).

The smaller cloud droplet sizes will likely lead to slower production of rain from conversion of cloud droplet, as well as subsequent growth of raindrops, such that the onset of nondrizzle precipitation might take longer in MG08 scheme. To verify this, we selected some grid points around the globe and examined the time series of precipitation produced by microphysics schemes (i.e., nonconvective precipitation) in

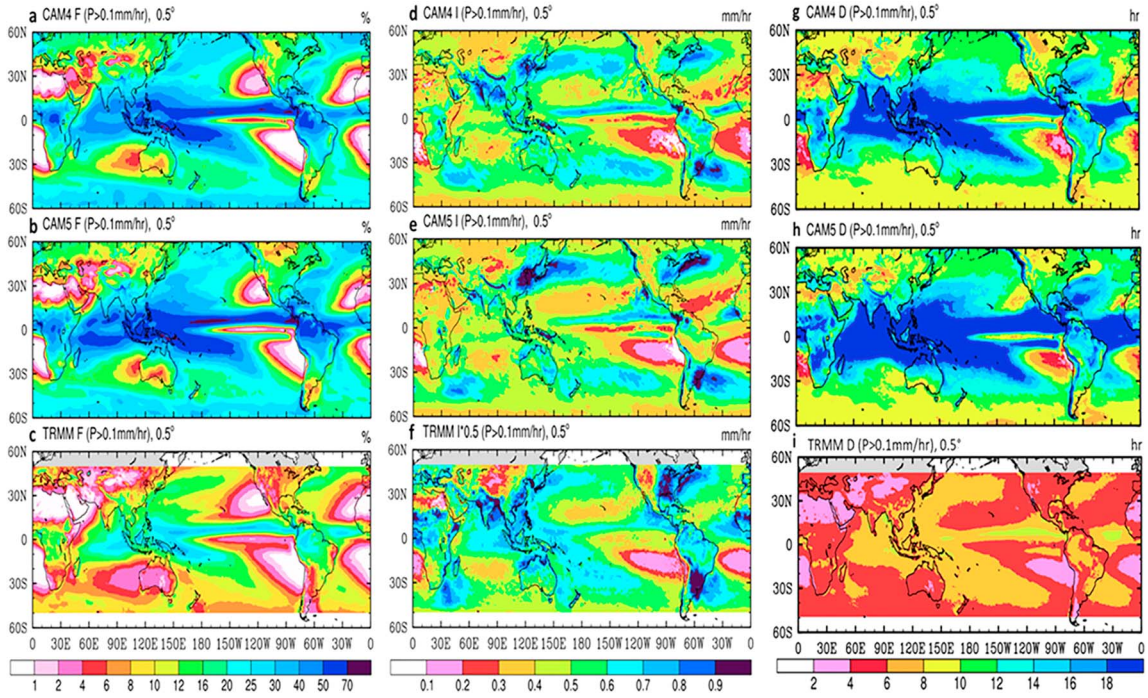

Figure 3. Mean precipitation (a–c) frequency (F in %), (d–f) intensity (I in mm/hr), and (g–i) duration (D in hours) estimated using 3-hourly total precipitation from (a, d, g) CAM4 and (b, e, h) CAM5 (on 0.47° lat × 0.63° lon resolution), and (c, f, i) from TRMM 3B42 data from 1998 to 2014 (averaged onto a 0.5° grid, the I in Figure 3f was multiplied by 0.5 for using the same color bar). CAM4 = Community Atmospheric Model version 4; CAM5 = Community Atmospheric Model version 5; TRMM = Tropical Rainfall Measuring Mission.

CAM4 and CAM5 (Figure 6). We found that there are less peaks of nonconvective precipitation in CAM5 (blue) than CAM4 (red), indicating it does take more time for the raindrops to grow, and the onset of precipitation events exceeding the 0.1 mm/hr (i.e., nondrizzle) thresholds is slower in MG08 scheme. These event-based diagnostics agree with the lower climatological frequency (Figure 4c) and amount (Figure 2b) of nonconvective precipitation in CAM5. Gettelman et al. (2008) also shows that the stratiform precipitation produced by the CAM3 physics with MG08 scheme is lower over the tropics and subtropics than with RK98 scheme. This reinforces our results that the microphysics schemes largely contribute to the difference of precipitation partition, despite substantial changes of other aspects from CAM4 to CAM5.

The next question is why does CAM5 produce more convective precipitation than CAM4 (Figure 2), given that they share the same deep convection scheme from Zhang and McFarlane (1995, hereafter *ZM95*). As shown in Figure 7a, the evaporative loss for raindrops is much higher in CAM5 than in CAM4. This difference mainly comes from evaporation of nonconvective precipitation, since evaporation of ZM95 convective precipitation (dash lines) is similar in CAM4 and CAM5. This likely results from the smaller droplet sizes produced by MG08 scheme, as smaller droplet sizes overall lead to larger rain evaporation rate (Morrison et al., 2009). The climatological convective available potential energy (CAPE, Figure 7b) is only slightly higher in CAM5, which is likely a result of the quasi-equilibrium assumption of the ZM95 scheme. It is reasonable to believe that more CAPE is consumed by the ZM95 scheme in CAM5, as convective precipitation is significantly higher in CAM5 than CAM4. Simulation outputs with higher temporal frequency (shorter than convective timescale) would be necessary to test this hypothesis, but it is beyond the scope of this study. On the other hand, it also makes sense since total precipitation, which is constrained by atmospheric energy balance (Pendergrass & Hartmann, 2014b), is similar in CAM4 and CAM5, thus CAM5 would generate more convective precipitation by the convection scheme to compensate for its lower nonconvective precipitation (Figure 2d) produced by the microphysics scheme. Other parameterization (e.g., PBL schemes, shallow convection schemes, and radiation packages) differences between CAM4 and CAM5 may also influence the partitioning of convective and nonconvective precipitation but are beyond the scope of this study.

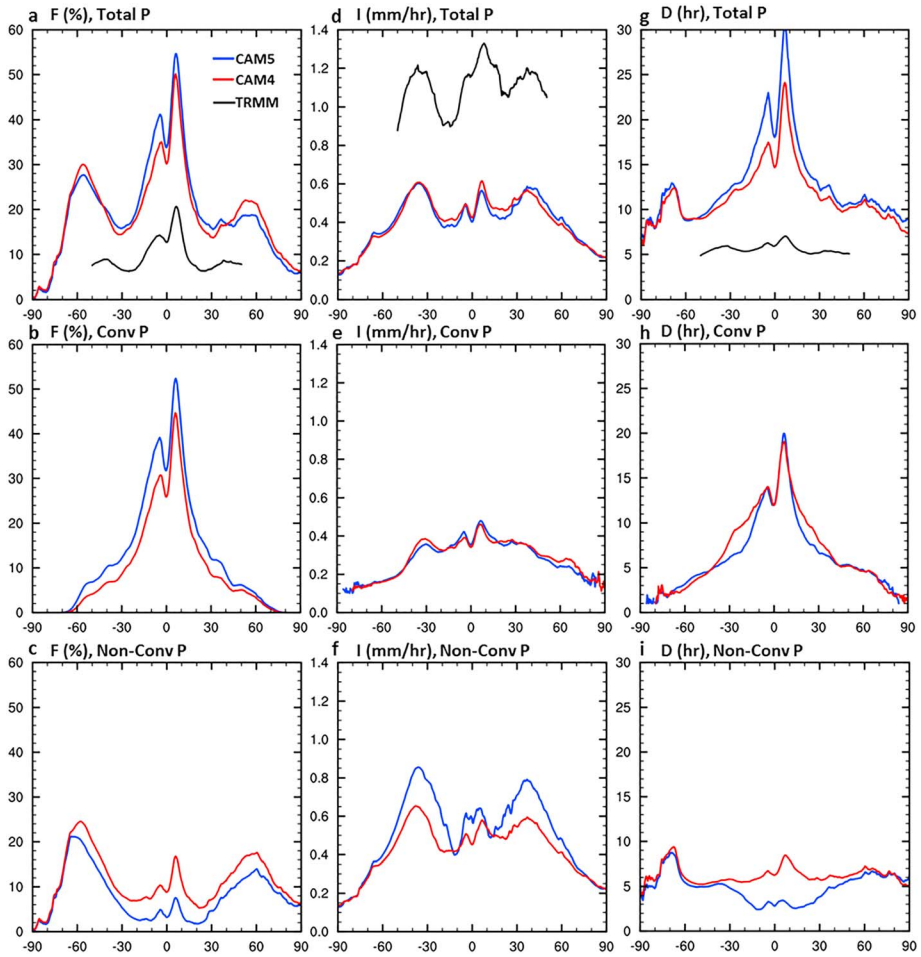

Figure 4. Zonal mean (a–c) frequency (F), (d–f) intensity (I), and (g–i) duration (D) of 3-hourly total precipitation, and of hourly convective and nonconvective precipitation from simulations using CAM4 and CAM5 on 0.47° lat × 0.63° lon resolution. The F, I, and D from TRMM 3B42 3-hourly precipitation averaged onto a 0.5° grid are shown as the black line in Figures 4a, 4d, and 4g for comparison. CAM4 = Community Atmospheric Model version 4; CAM5 = Community Atmospheric Model version 5.

3.2. Resolution Dependence

The estimated precipitation F, I, and D are dependent on horizontal resolutions of the input data (Benedict et al., 2017; Chen & Dai, 2018). The CAM simulations with varying resolutions provide a good opportunity to further investigate this issue. Here we examine both the effects from pure area aggregation (Chen & Dai, 2018) and adjustments of the model physics and dynamics to changing resolutions mainly using CAM4 simulations on 0.23° × 0.31°, 0.47° × 0.63°, 0.9° × 1.25°, and 1.9° × 2.5° (abbreviated as 0.25, 0.5, 1.0, and 2.0°, respectively) grids. CAM5 results will also be discussed for comparison.

3.2.1. Precipitation Amount

Figure 8 compares precipitation A, F, I, and D simulated by CAM4 on the 0.25 and 2.0° grids. Figures 8a and 8b show very similar distributions of total precipitation amount, although noticeable regional differences exist, for example, over the Indian Ocean and North Pacific (which may partly result from sampling errors due to the relatively short simulations). Zonal mean total precipitation amount varies little with horizontal resolution, although finer resolutions (e.g., 0.25°) produce a sharper peak with higher precipitation over the ITCZ and the South Pacific Convergence Zone, and more precipitation over the midlatitudes than the 2° simulation (Figure 9a). In contrast, the partitioning between the convective and nonconvective precipitation (Figures 9b–9d) is sensitive to the resolution change, with a coarse resolution (e.g., 2.0°) producing more convective but less nonconvective precipitation than a fine grid,

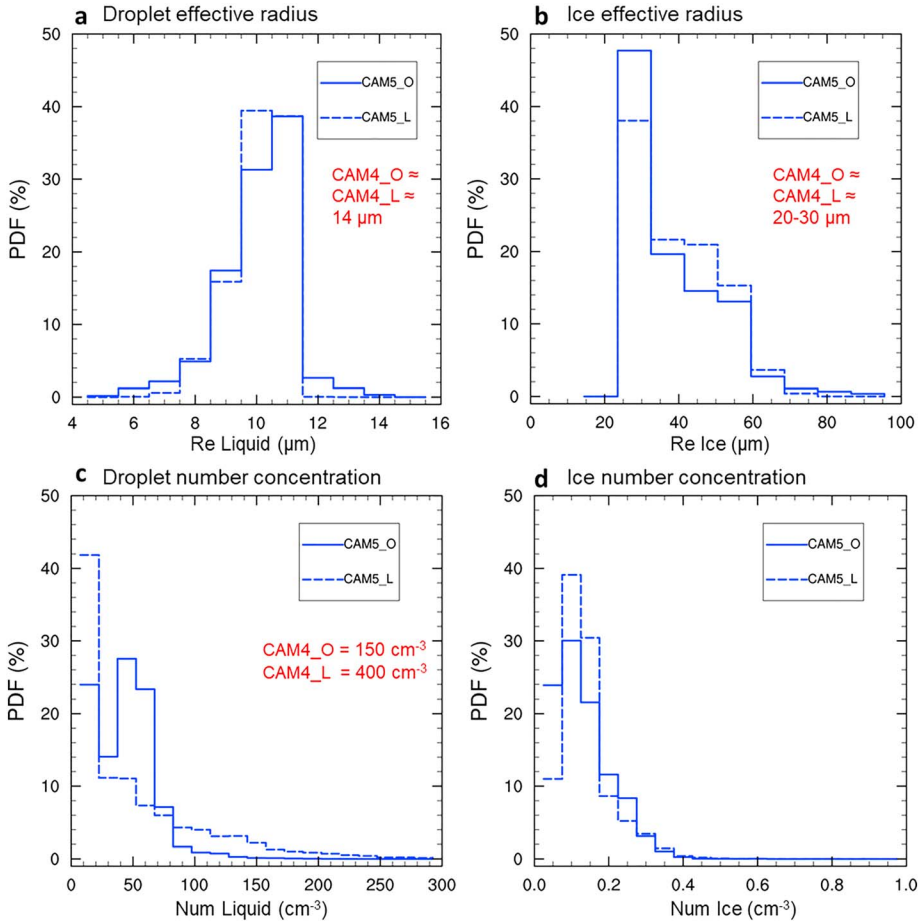

Figure 5. PDFs of tropospheric (950–100 hPa) (a) cloud droplet (liquid) and (b) cloud ice effective radius (Re), (c) in-cloud droplet, and (d) in-cloud ice number concentration (Num) in CAM5 (blue) over land (dash) and ocean (solid). The calculation follows Gettelman et al. (2008). The specified values in CAM4 (Neale et al., 2010) are shown in red. The CAM4 and CAM5 outputs with 0.9° lat × 1.25° lon resolution are used. PDFs = probability density function; CAM4 = Community Atmospheric Model version 4; CAM5 = Community Atmospheric Model version 5.

and the convective-to-total precipitation ratio increases with the grid size (Figure 9d). This difference is also evident over major mountain ranges such as the Himalayas, the Rocky Mountains, and the Andes. Smaller grid sizes allow better representation of the mesoscale systems, whose trailing stratiform section usually spans ~100 km (Houze, 2004), leading to higher resolved (i.e., nonconvective) precipitation from the cloud microphysics scheme and a smaller role of the convection parameterization for subgrid convective precipitation, as noticed previously (e.g., Bacmeister et al., 2014; Kooperman et al., 2018). Convective and nonconvective precipitation act to compensate with each other, leading to smaller resolution dependence of total precipitation. CAM5 also produces more convective precipitation and less nonconvective precipitation as the grid size increase from 0.5 to 1.0 and to 2.0°, although these changes are slightly smaller than in CAM4.

3.2.2. Precipitation Frequency, Intensity, and Duration

Similar to the resolution dependence seen in observational precipitation (Chen & Dai, 2018), CAM-simulated precipitation F increases and I decreases as the grid size increases over most low-middle latitudes (Figures 10a and 10d), especially over the ITCZ and most land areas (Figures 8c–8f). At a finer resolution, CAM4 produces more intense precipitation over the equatorial Pacific and major monsoon regions such as India, East Asia, and South America (Figures 8e and 8f). Precipitation over the Himalayas and the Andes also becomes more intense on the 0.25° grid than on the 2.0° grid. The frequency of convective precipitation (Figure 10b) has a resolution dependence similar to that for total precipitation over the tropics, while its intensity has slightly weaker dependence (Figure 9e). The

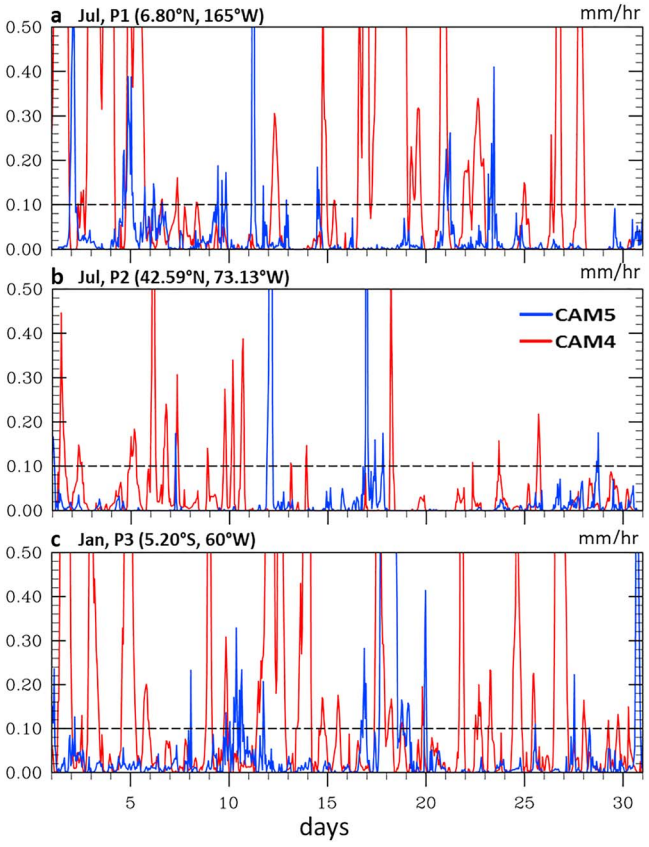

Figure 6. (a–c) Time series of nonconvective precipitation (from the cloud microphysics scheme) for three selected locations over an arbitrary month. The 0.1 mm/hr threshold for nondrizzle precipitation is indicated by the thin dashed line. The CAM4 (red) and CAM5 (blue) outputs with 0.47° lat × 0.63° lon resolution are used. CAM4 = Community Atmospheric Model version 4; CAM5 = Community Atmospheric Model version 5.

relationship is reversed for nonconvective precipitation: finer grids yield slightly higher F (especially around 7°N, Figure 10c), which can be attributed to the fact that finer resolutions resolve more larger-scale features of mesoscale systems and produce more precipitation (at the expense of parameterized precipitation from the convection scheme). The intensity of nonconvective precipitation (Figure 10f) increases greatly as the grid size becomes smaller. One interesting feature is that the resolution dependence for F is very weak over the high latitudes, as convective precipitation rarely occurs there while nonconvective precipitation shows small resolution dependence at high latitudes (Figures 10a–10c). Satellite products do not cover the high latitudes (Chen & Dai, 2018), thus we do not know if that is the case in the real world.

Precipitation duration (D) is also highly sensitive to model resolution. The duration of all precipitation events on the 2° grid (Figure 8h) is over 28 hr over the tropical oceans, which is much higher than the duration of 8–12 hr over these areas on the 0.25° grid (Figure 8g). The duration of all precipitation events on the 0.25° grid (Figure 10g) is comparable with that from TRMM (although it is 2–4 hr longer over the tropics); but as grid size increases to 2.0°, the D becomes much longer, especially around 7°N. Outside the tropics, the D is generally doubled from the 0.25 to 2.0° resolution. Most of the low-middle latitude D features come from convective precipitation (Figure 10h), which is expected as convective precipitation dominates over nonconvective precipitation at the low-middle latitudes (Figure 2c). The duration of nonconvective precipitation (Figure 10i) also increases with the grid size, although with a slower rate. Precipitation duration in CAM5 is similar to CAM4 on the 0.5° grid but is shorter than CAM4 at coarser resolutions.

3.2.3. Decomposing Resolution Dependence in CAM

Can the pure area aggregation discussed in Chen and Dai (2018) alone explain the resolution dependence in CAM? Do other factors, such as

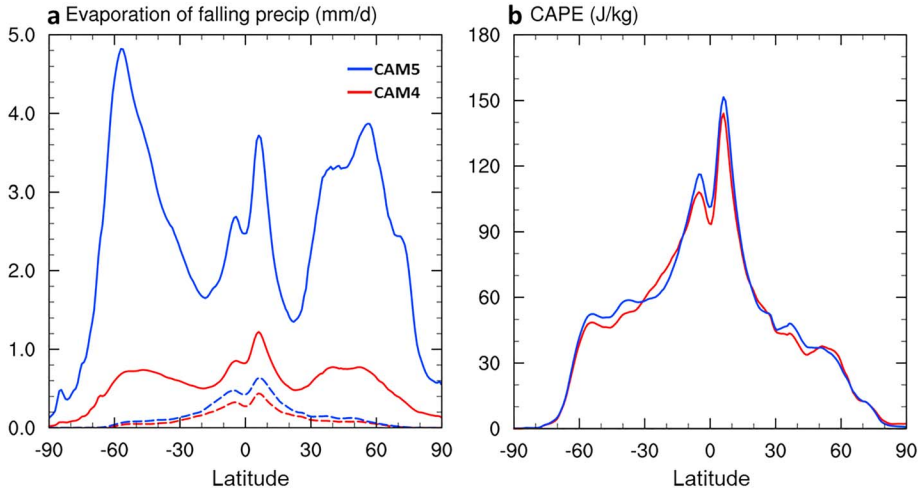

Figure 7. Zonal mean annual (a) evaporative loss of total falling precipitation (mm/day, solid lines) and evaporative loss of convective precipitation from Zhang and MacFarlane scheme (mm/day, dash lines) in CAM4 and CAM5. (b) Convective available potential energy (CAPE, J/kg) in CAM4 (red) and CAM5 (blue). The CAM4 and CAM5 outputs with the 0.9° lat × 1.25° lon grid were used. CAM4 = Community Atmospheric Model version 4; CAM5 = Community Atmospheric Model version 5.

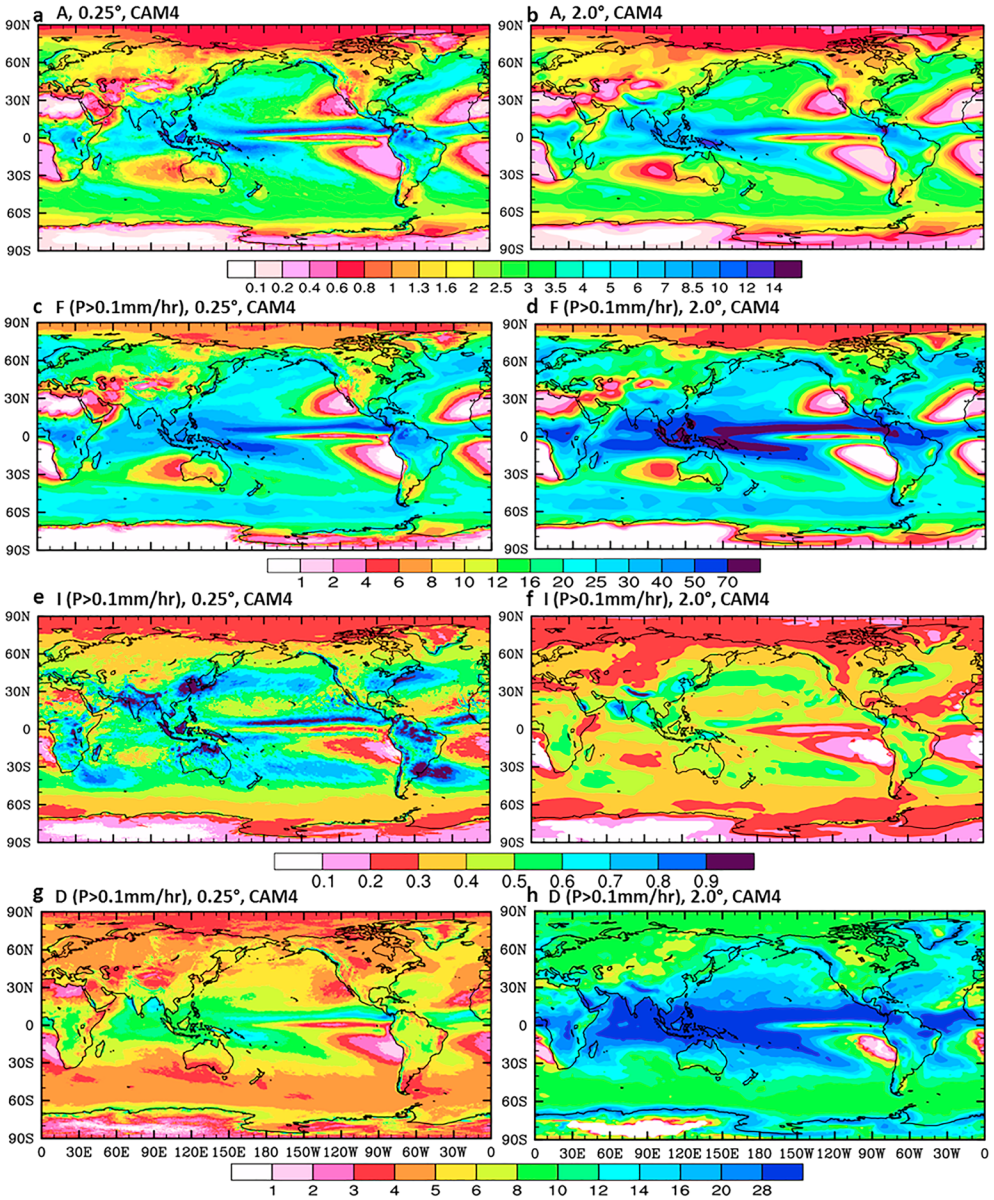

Figure 8. Mean annual total precipitation (a and b) amount (A), (c and d) frequency (F), (e and f) intensity (I) and duration (D) estimated using CAM4 outputs on 0.23° lat × 0.31° lon (0.25°, left) and 1.9° lat × 2.5° lon (2.0°, right) grids. Only nondrizzle precipitation events with $P > 0.1$ mm/hr were included in computing the F, I, and D. CAM4 = Community Atmospheric Model version 4.

the resolution dependence of the model physics and model-simulated atmospheric circulation (all referred to as model adjustments to resolution), contribute to the resolution dependence discussed above? In order to answer these questions, following the method of Chen and Dai (2018), we first spatially averaged the CAM4 precipitation on the 0.25° resolution onto the 0.5, 1.0, and 2.0° resolution (referred to as the aggregated precipitation) and then calculated the F, I, and D on each of these grids, which are shown in Figure 11. From 0.25 to 2.0° resolution, area aggregation leads to an increase of about 10% (4%) in the F within 10°S–10°N (outside 10°S–10°N) for total, convective, and nonconvective precipitation (Figure 11a–11c). For intensity, area aggregation leads to a decrease of about 0.2 mm/hr within 45°S–45°N for all types of precipitation. Area aggregation also increases the D by 4–14 hr from the 0.25 to 2.0° grid, and the D increase is especially large for total and convective precipitation at low latitudes (Figures 11g–11i). We notice that the aggregation effect from 0.25 to 0.5° is very small. This is likely

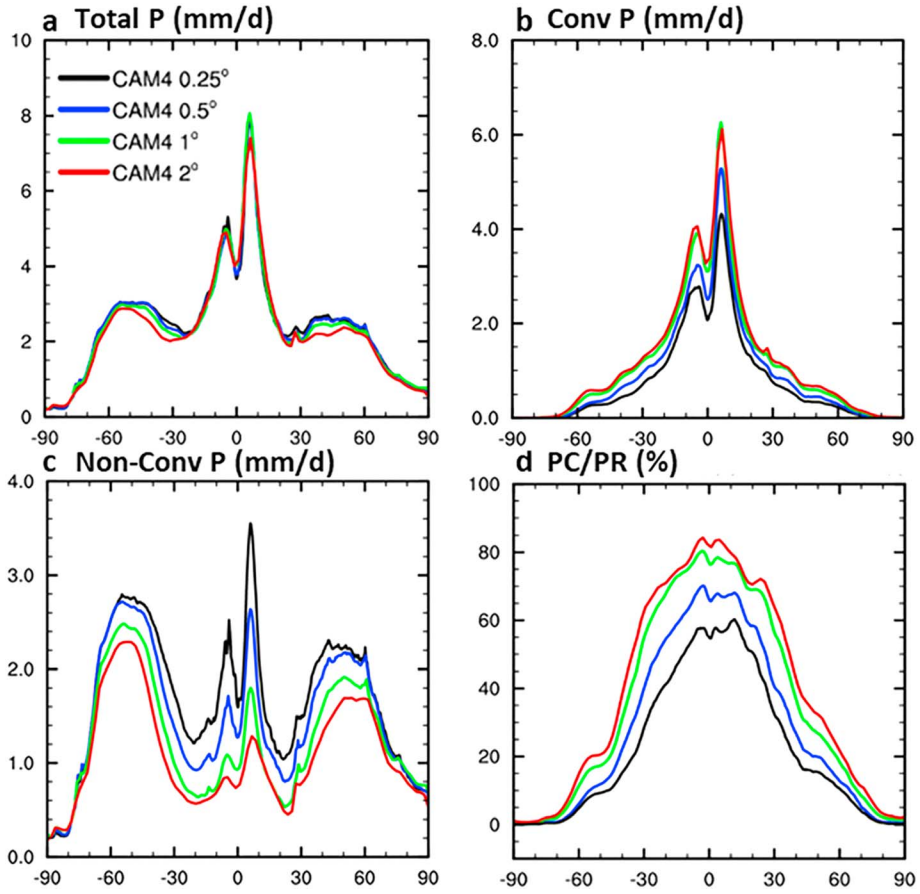

Figure 9. Zonal mean annual (a) total, (b) convective (Conv) and (c) nonconvective (Non-Conv) precipitation amount, and (d) convective-to-total precipitation (PC/PR) ratio produced by CAM4 on four different spatial resolutions (0.23° lat × 0.31° lon, 0.47° × 0.63°, 0.9° × 1.25°, and 1.9° × 2.5°). CAM4 = Community Atmospheric Model version 4.

due to the high spatial correlation of precipitation in CAM4 at small distances (see below), which means that precipitation over nearby 0.25° grid boxes tends to occur almost always at the same time, leading to little aggregation effect from 0.25 to 0.5° grids.

To remove the area aggregation effect, we averaged the hourly precipitation from the 0.25, 0.5, and 1.0° CAM4 simulations onto the same 2.0° grid used in the 2.0° CAM4 simulation and then calculated the F, I, and D, which are shown in Figure 12. Since these properties were derived from the data with the same spatial and temporal resolution, their differences (Figure 12) represent the impact from the model adjustments to different resolutions (on the F, I, and D estimated on the 2.0° grid). In comparison with Figures 10 and 11, Figure 12 shows that the effect from the model adjustments is smaller than that due to the area aggregation, but still is considerable, especially for the D of convective precipitation and I of the nonconvective precipitation; and it roughly enhances the differences caused by the area aggregation, leading to larger differences in the combined effects shown in Figure 10. The model adjustments (mainly through the convection scheme) increase the F and D (and also slightly for A, Figure 9b) of convective precipitation as the grid size increases, but reduce the F and I and also A (Figure 9c) of the model-resolved nonconvective precipitation. As mentioned above, as the grid size increases, more mesoscale precipitation processes become unresolved and need to be accounted for by the subgrid parameterization (i.e., the convective scheme), leading to more frequent and longer (due to the larger spatial scales) precipitation events and thus more total convective precipitation; while the number and intensity of the resolved precipitation events should decrease as fewer precipitation events (especially small scale intense storms) are resolved on coarse grids. When we subtracted the 0.25° case (black line) from the other colored lines in Figure 12 and added this difference (resulting from the model adjustments) to Figure 11 (resulting from the area aggregation), the results (not shown) are very similar to

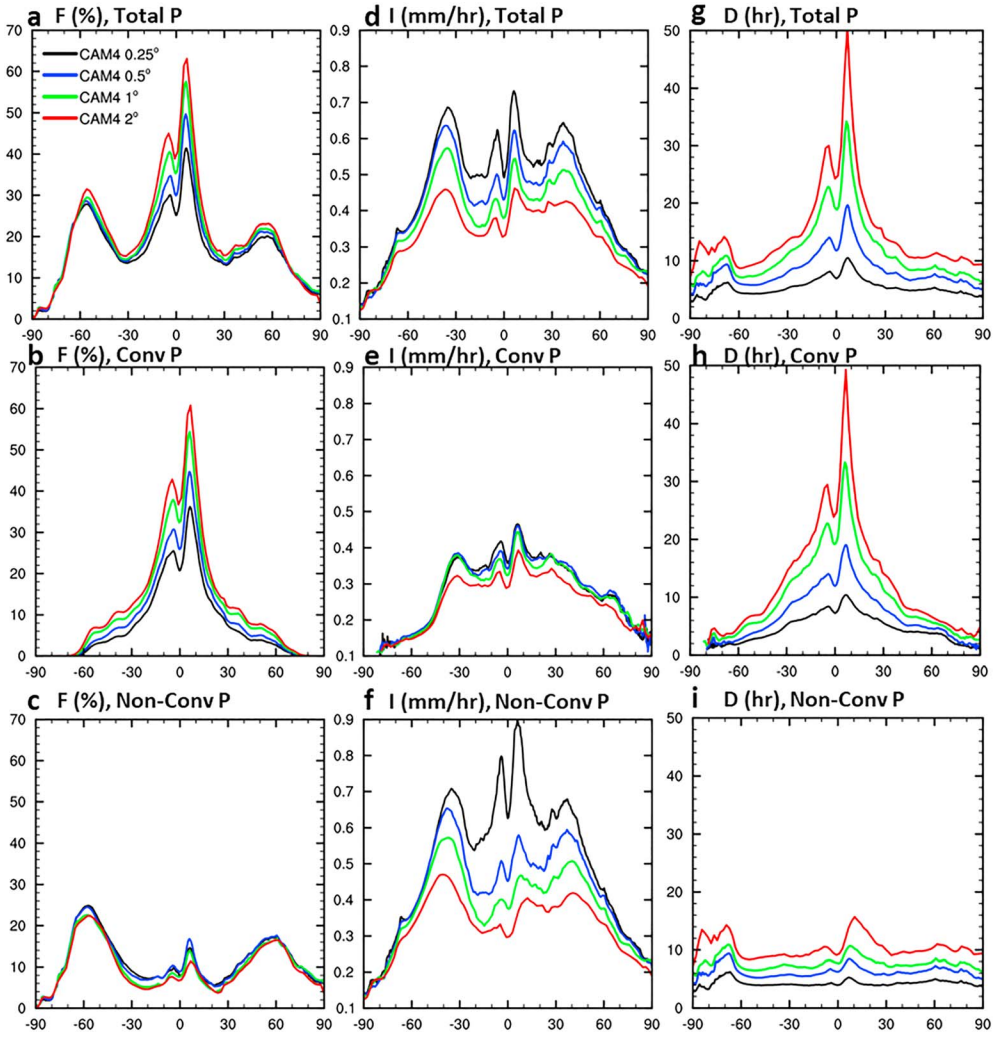

Figure 10. Zonal mean (a–c) frequency (F, in %), (d–f) intensity (I, in mm/hr), and (g–i) duration (D, in hours) of total, convective, and nonconvective precipitation estimated using hourly precipitation data from simulations using CAM4 with four different spatial resolutions. Only nondrizzle precipitation events with $P > 0.1$ mm/hr were included in computing the F, I, and D. CAM4 = Community Atmospheric Model version 4.

Figure 10. These suggest that the resolution dependence of the precipitation characteristics in CAM4 results primarily from the area aggregation effect but is enhanced considerably by the model adjustments to different resolutions, and the model adjustments result mainly from the increased (decreased) subgrid convective (resolved nonconvective) precipitation as the grid size increases.

The combined effects of the area aggregation and model adjustments in CAM produce a weaker resolution dependence for F (Figure 13a) than that seen in observational data (Chen & Dai, 2018). The scaling ratio (SR = F (coarse gird)/F (fine grid), Chen & Dai, 2018) measures the resolution dependence quantitatively, with higher SR indicating stronger resolution dependence. Figure 13a shows that the SR is significantly lower in CAM4 than in TRMM, especially for the 2.0 versus 0.25° case (solid lines). If excluding the effect of model adjustments and considering the area aggregation effect only (as is the case for the TRMM data), the SR for CAM4 (blue lines in Figure 13a) is even lower at low latitudes. As mentioned above, the aggregation effect from 0.25 to 0.5° (dashed blue line in Figure 13a) is small, while it accounts for about half of the total F increase from 0.25 to 2.0° seen in CAM4 at the low latitudes (blue and red solid lines in Figure 13a).

The low SR in CAM4 is related to its high spatial covariability in precipitation, that is, the high probability for a grid point to have precipitation at the same time with its surrounding grid points. This probability can

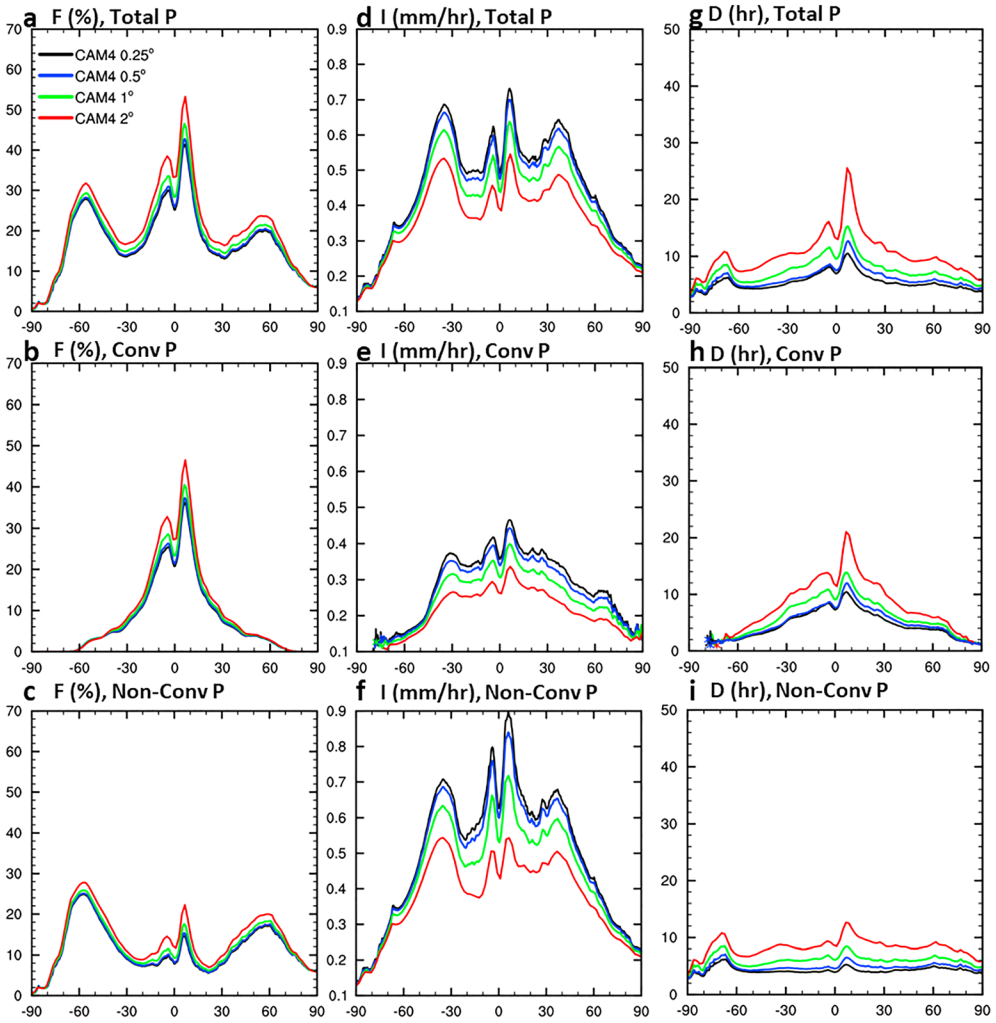

Figure 11. Zonal mean (a–c) frequency (F, in %), (d–f) intensity (I, in mm/hr), and (g–i) duration (D, in hours) of total, convective, and nonconvective precipitation estimated using hourly precipitation data from the 0.25° CAM4 simulation (black line) and using the same hourly data but averaged onto the 0.5, 1.0, and 2.0° grid to derive the F, I, and D for the latter three resolutions. Only nondrizzle precipitation events with $P > 0.1$ mm/hr were included in computing the F, I, and D. CAM4 = Community Atmospheric Model version 4.

be quantified by the simultaneous correlation of precipitation between a given point and its surrounding points, as shown in Figures 13b–13d and also examined by Trenberth and Zhang (2018b). Figures 13b–13d show that spatial correlations of precipitation are significantly higher in CAM4 than in TRMM, and the correlation is close to 1.0 for a separation distance of ≤50 km, which explains why the area aggregation effect is small from 0.25 to 0.5° grid. The high spatial correlation in CAM4 suggests that precipitation tends to occur simultaneously over a large area, leading to less increase of precipitation probability over a larger sampling area, that is, precipitation frequency in CAM4 should be less susceptible to the area aggregation effect than in TRMM. These diagnostics illustrate that precipitation in CAM4 and CAM5 differ substantially from reality in terms of the temporal and spatial characteristics. Trenberth et al. (2017) found that precipitation tend to be more episodic and intermittent in the real world than in CAM. Precipitation spatial variations over short distances are also larger in observations than in CAM (Trenberth & Zhang, 2018b). The sizes of precipitating systems tend to be larger and more homogeneous in CAM than in observations. We believe that correctly simulating the temporal and spatial features of precipitating system may be a key to improving the simulated precipitation characteristics. Additionally, the large SR difference at low latitudes in CAM4 between the cases with (red lines) and

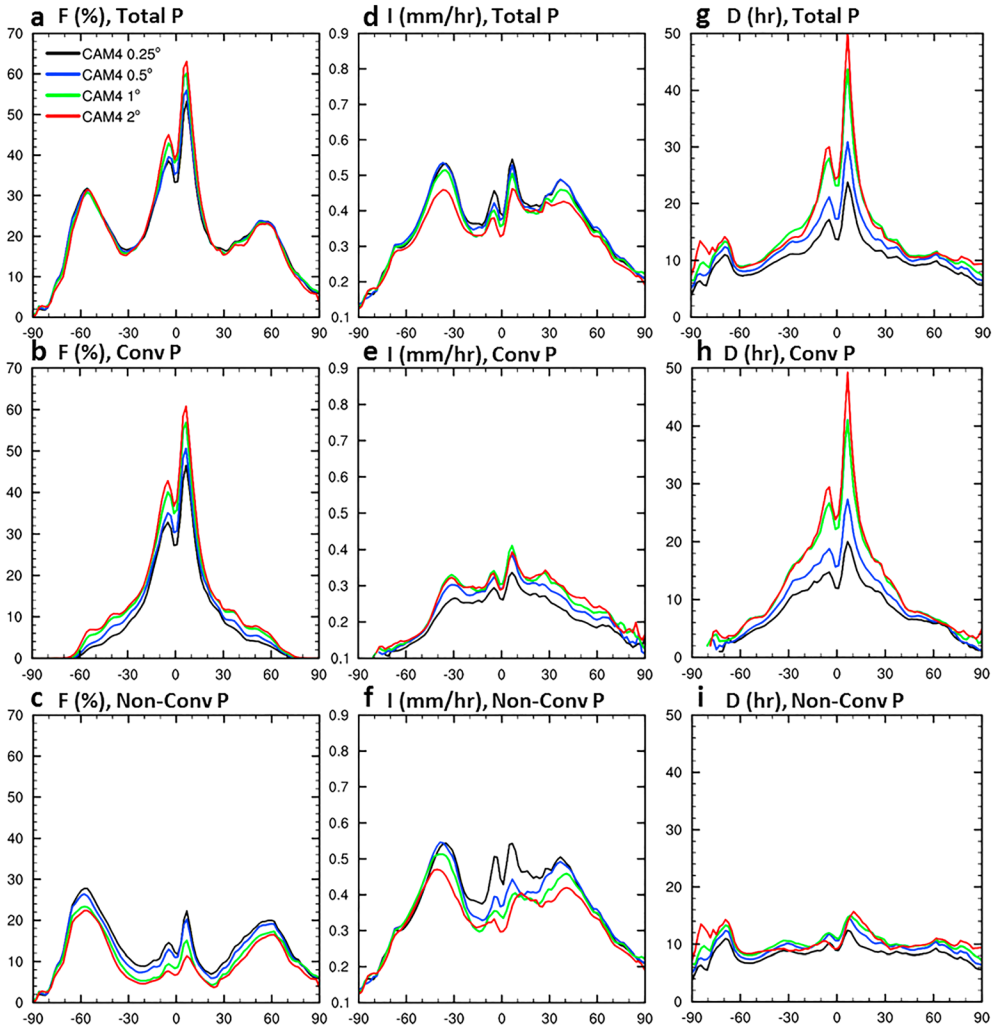

Figure 12. Zonal mean (a–c) frequency (F, in %), (d–f) intensity (I, in mm/hr), and (g–i) duration (D, in hours) of total, convective, and nonconvective precipitation estimated using hourly precipitation data averaged onto the same 2.0° grid using the hourly output from CAM4 simulations with four different spatial resolutions (no averaging for the 2° case). Only nondrizzle precipitation events with $P > 0.1$ mm/hr were included in computing the F, I, and D. CAM4 = Community Atmospheric Model version 4.

without (blue lines in Figure 13a) the model adjustments again indicates significant effects from model adjustments.

As mentioned above, the key process involved in the model adjustments is that the resolved precipitation events (by the cloud microphysics scheme) are a strong function of the grid size and therefore should become fewer as the grid size increases, while the parameterized precipitation events (through the convection scheme) should cover an increasing range of spatial scales and therefore should increase for larger grid sizes (Bacmeister et al., 2014; Rauscher et al., 2016). Other processes, such as better-resolved orographic precipitation and other regional circulation features in finer grids, may also play a role. Besides, several aspects of the convective parameterization can affect total precipitation partition (Sakaguchi et al., 2018; Williamson, 2013; Yang et al., 2013), notably time step changes associated with resolution change. Williamson (2013) suggests that when the model time step is lengthened, convective parameterization will be more active hence more convective precipitation is produced. This is largely due to the mismatch between the model time step and the convective timescale of the deep convection scheme (Gustafson et al., 2014; Ma et al., 2014; Williamson, 2013). The convective timescale of Zhang and McFarlane (1995) scheme is fixed to 3,600 s in all simulations. For our CAM4 and CAM5 simulations, the physics time step is the same at 1800 s for the

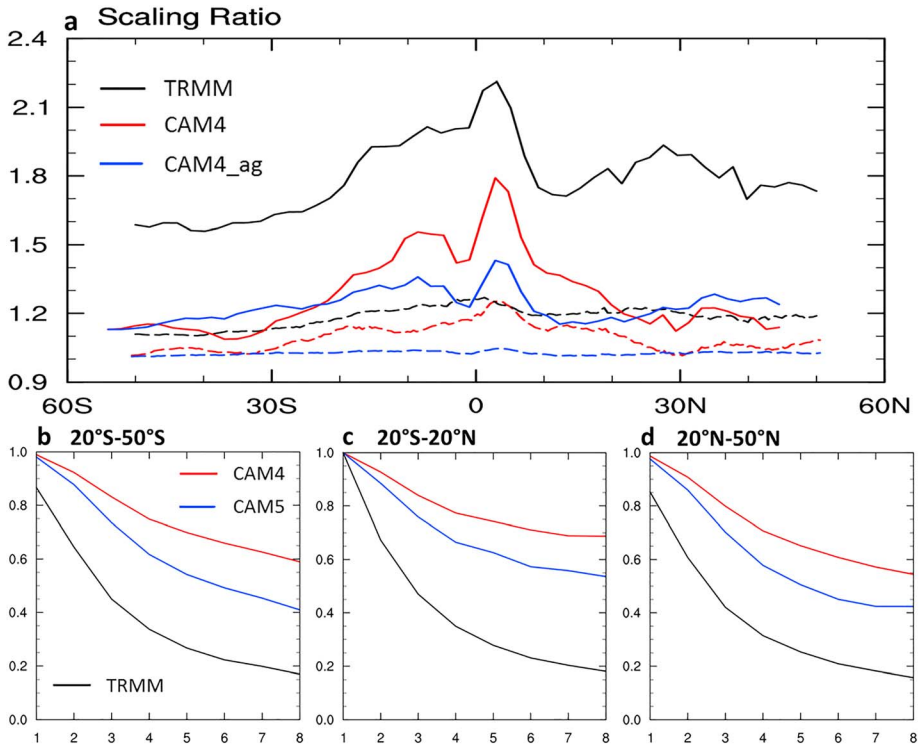

Figure 13. (a) Zonal mean scaling ratio (SR) of precipitation frequency between the 2.0 and 0.25° grids (solid lines) and between the 0.5 and 0.25° grids (dashed lines) derived using 3-hourly data from TRMM 3B42 (black) and CAM4 simulations (red). The blue lines are for the frequency ratio derived using the grid-averaged precipitation by averaging the data on the 0.25° grid onto the 2.0 or 0.5° grid; thus, it reflects only the aggregation effect (as for the TRMM case). The red lines include the combined effects from the area aggregation and model adjustments. Zonally averaged spatial correlations of 3-hourly precipitation on 0.5° grid as a function of the separation distance (in units of 50 km) from TRMM 3B42 (black), CAM4 (red), and CAM5 (blue) for (b) 20–50°S, (c) 20°S–20°N, and (d) 20–50°N. CAM4 = Community Atmospheric Model version 4; CAM5 = Community Atmospheric Model version 5; TRMM = Tropical Rainfall Measuring Mission.

0.5, 1.0, and 2.0° grids but is reduced to 900 s for the 0.25° grid. Thus, most of the differences shown in Figures 9 and 10 are not related to this time step effect, except the case of the 0.25° grid, whose difference from the other grids may contain some effect from the time step change. In addition, the F is overall less resolution dependent in CAM5 than CAM4. This is likely to due to the more consistent behavior of stratiform clouds and precipitation produced by the MG08 microphysics scheme across resolutions (O'Brien et al., 2013).

4. Conclusions and Discussion

We have performed and analyzed a series of simulations with varying grid spacing using CAM4 and CAM5 forced by monthly SST climatology to systematically investigate the resolution dependence of precipitation amount (A), frequency (F), intensity (I), and duration (D), with a focus on the difference between parameterized (convective) and resolved (nonconvective) precipitation. We also have examined the impact of the different model physics in the two versions of the CAM model and the effect from the adjustment of model physics to varying model resolutions. It is found that all four characteristics (A, F, I, and D) depend on model horizontal resolution to a varying degree, although the total (convective plus nonconvective) precipitation amount is not sensitive to model resolution and model physics. Large differences exist in the F, I, and D for the convective and nonconvection precipitation, which implies that incorrect partitioning between these two types of precipitation may lead to biases in the simulated precipitation F, I, and D. The F and D (I) increase (decreases) with model grid size, and this resolution dependence results primarily from the area aggregation effect with secondary contribution from the model adjustment effect, which also leads to higher F and D but lower I as the grid size increases. Substantial differences are also found in the F, I, and D

between CAM4 and CAM5, and different microphysics schemes likely have played a big role for these differences. Furthermore, the precipitation characteristics in CAM5 exhibit slightly weaker resolution dependence than in CAM4. Below is a more detailed summary.

Total precipitation A in CAM4 and CAM5 shows realistic spatial distributions and seasonal variations in comparison with the GPCP climatology, although they slightly overestimate the A over the ITCZ, as shown previously (Bacmeister et al., 2014; Dai, 2006; DeMott et al., 2007; Flato et al., 2013). However, CAM4 and CAM5 differ significantly on the partitioning of convective (from the convection scheme) and nonconvective (from the cloud microphysics scheme) precipitation. CAM5 produces more convective precipitation while CAM4 has more nonconvective precipitation, resulting in slightly more total precipitation in CAM5, as noticed previously (Bacmeister et al., 2014). The convective-to-total precipitation (PC/PR) ratio in CAM5 is about 0.2 higher than that in CAM4 over the tropics, where the PC/PR ratio is unrealistically high in both models (PC/PR = 0.8–0.9 in CAM5 and 0.6–0.7 in CAM4 with 0.5° resolution but decreases to 0.5–0.6 with 0.25° resolution in CAM4) in comparison with TRMM (~0.4–0.5 on 0.25° grid, Figure 2), a common bias in many older climate models (Dai, 2006). We acknowledge that the definitions of nonconvective (or stratiform) precipitation are not directly comparable between CAM and TRMM 3A25, as CAM partitions precipitation by the convection and cloud microphysics schemes, whereas TRMM classifications are based on radar bright band and reflectivity. Recent implementation of cloud simulator in models (e.g., Kay et al., 2018) might help bridge the gap. Nevertheless, we show that the partitioning reflects key aspects of model precipitation physics, and it has major implications for the overall characteristics of the simulated precipitation. Our results (Figure 9) suggest that this bias of overestimating convective precipitation is at least partly due to the use of coarse grid spacing in global models (consistent with Bacmeister et al., 2014), which fail to resolve many regional to mesoscale precipitation events (as resolved precipitation) and have to rely on the convection parameterization to simulate these events in the form of parameterized convective precipitation. Given the large differences in the F, I, and D between the convective and nonconvective precipitation in CAM (Figure 10), such a bias in the PC/PR ratio would result in major biases in the model-simulated F, I, and D.

Indeed, the reasonable precipitation A comes from incorrect combinations of precipitation F (too high) and I (too low) in CAM4 and CAM5, again a common problem in many older climate models (Dai, 2006). Both versions of CAM substantially overestimate precipitation F and D while underestimating I. The F in CAM (up to 60–70% in the ITCZ) is much higher than that in TRMM (up to 30% in the ITCZ, both on a 0.5° grid), while CAM produces less than half of the intensity seen in TRMM. The D in CAM over the tropics is 6–12 hr longer than and about twice of that seen in TRMM. While our results (Figure 11) suggest that part of these F, I, and D biases may result from the use of coarse grid spacing in climate models, the resolution dependence alone cannot account for all of these biases in F, I, and D (Figure 4). One additional source of these biases is the unrealistically high convective precipitation, which has higher F and D but lower I than those of the nonconvective precipitation (Figure 10). Thus, one way to reduce the F, I, and D biases is to allow the microphysics scheme to produce more precipitation (e.g., by reducing its evaporative loss of raindrops, Figure 7), which would decrease the overall frequency and duration while increasing the intensity. Meanwhile, reducing the precipitation produced by the convection scheme may also improve the overall precipitation characteristics. From this perspective, CAM5 might be a step backward from CAM4, as it produces more convective precipitation and less nonconvective precipitation than CAM4 (Figure 2), resulting in even higher F and D than in CAM4 (Figure 4). On the other hand, the MG08 scheme in CAM5 produces more realistic cloud particles size and number concentration than CAM4 (Gettelman et al., 2008). Given this improvement, the above mentioned bias (i.e., more light precipitation) in CAM5 may be due to the formulation of evaporative loss of raindrops, rather than the size distributions.

In general, nonconvective precipitation needs to increase while convective precipitation needs to decrease in both CAM4 and CAM5. Bacmeister et al. (2014) suggested that the convection parametrization of CAM is overly active in producing weak-to-moderate precipitation. Here we show that this problem is likely more severe in CAM5. Previous studies (e.g., Held et al., 2007; Pendergrass & Hartmann, 2014b) based on other climate models such as the GFDL-ESM-2G also suggest that resolved precipitation is more intense than parameterized precipitation. Kooperman et al. (2018) also recommended that linking resolved large-scale processes more directly to mechanisms controlling total precipitation production would likely produce more realistic moderate precipitation rates. An alternative way to improve the

overall precipitation characteristics is to decrease the F and D while increase the I of convective precipitation alone. For instance, a larger entrainment rate in the ZM95 scheme may help the development of deep and intense convection in CAM (DeMott et al., 2007), which should produce more intense convective precipitation. Insights from observational studies on both types of precipitation, along with more consistent and physical depiction of them in GCMs, would improve the A, F, I, and D of precipitation in models for right reasons.

The difference in cloud microphysics schemes is likely a major contributor to the differences in the simulated precipitation characteristics between CAM4 and CAM5. We found the CAM5 microphysics (MG08) scheme produces significantly smaller effective radius of cloud and ice particles (Figure 5) than the CAM4 microphysics (RK98) scheme, similar to previous study using CAM3 (Gettelman et al., 2008). We showed that the onset of precipitation events exceeding the 0.1 mm/hr (i.e., nondrizzle) thresholds is slower in MG08 scheme (Figure 6), which likely results from the smaller cloud droplet sizes and hence slower production of rain. The slower onset and less occurrence of nondrizzle events lead to lower climatological frequency and amount of nonconvective precipitation in CAM5 than in CAM4. We also show that the smaller droplet sizes in CAM5 induce higher evaporative loss for raindrops (Figure 7a), while more moisture may be consumed by the deep convection scheme in CAM5, although the climatological CAPE is not significantly higher in CAM5 than CAM4 (Figure 7b). Therefore, the improvements in-cloud particle size distributions produced by MG08 scheme should be accompanied by other improvements such as better formulation of evaporation to achieve better overall results. Other parameterizations between CAM4 and CAM5 cloud also influence the simulated precipitation but are beyond the scope of this study.

The model-simulated precipitation characteristics are found to be sensitive to model resolution, although the difference of the 0.25° grid from the other grids may also contain some effects from a time step change. Consistent with Chen and Dai (2018), precipitation F and D in CAM decreases as the grid size decreases, especially for convective precipitation; while precipitation I increases as the resolution increases, especially for nonconvective precipitation (Figure 10). Overall, the simulated A, F, and D are less sensitive to resolution in CAM5 than in CAM4. Further analyses show that the effect of area aggregation discussed in Chen and Dai (2018) can explain a large part of the resolution dependence. Different performances of model physics and model dynamics under varying resolutions (referred to as model adjustments) account for a significant part of the resolution dependence at low latitudes seen in the CAM simulations. In general, the model adjustments increase the F and D for convective precipitation but decrease the F and I for nonconvective precipitation, with the largest impacts on the D under coarser resolutions and over the tropics (Figure 12). In addition to increasing nonconvective and reducing convective precipitation as shown here and previously (e.g., Bacmeister et al., 2014), finer resolutions can also enhance the intensity of vertical motion, change the resolved cloud fraction (O'Brien et al., 2016; Rauscher et al., 2016), and better resolve orographic precipitation. Furthermore, we show that spatial correlations of precipitation are too strong in CAM and this reduces the area aggregation effect for CAM precipitation, leading to CAM's lower-resolution dependence than that seen in TRMM.

Our results clearly show that finer resolutions are desirable for improved precipitation characteristics in climate models because they not only improve the partitioning between resolved and parameterized precipitation but also reduce the area aggregation effect, both leading to lower frequency and higher intensity for precipitation and thus alleviating the long-standing drizzling problem in global models (Dai, 2006). However, whether the CAM-based results reported here hold for other climate models remains to be seen, especially regarding the different F, I, and D between the resolved and parameterized precipitation and the impact of model adjustments to changing resolution.

Acknowledgments
We thank Brian E. J. Rose for his assistance in setting up the CESM1 simulations and Robert Fovell for constructive discussions on cloud microphysics schemes. We also thank two anonymous reviewers for comments that helped to considerably improve the manuscript. Dai acknowledges the funding support from the U.S. National Science Foundation (grant AGS–1353740 and OISE-1743738), the U.S. Department of Energy's Office of Science (Award DE–SC0012602), and the U.S. National Oceanic and Atmospheric Administration (Award NA15OAR4310086). The hourly CAM output is available through http://www.atmos.albany.edu/student/dchen/. The TRMM 3B42, TRMM 3A25, and GPCP v2.2 data are provided by the NASA GSFC. The TRMM 3B42 and TRMM 3A25 are available at https://pmm.nasa.gov/data-access/downloads/trmm, and the GPCP v2.2 is available at http://precip.gsfc.nasa.gov/.

References

Awaka, J., Iguchi, T., Kumagai, H., & Okamoto, K. (1997). Rain type classification algorithm for TRMM precipitation radar. In *Geoscience and Remote Sensing, 1997: IGARSS'97, Remote Sensing—A scientific vision for sustainable development* (Vol. 4, pp. 1633–1635). New York: Inst. of Electr. and Electron. Eng. https://doi.org/10.1109/IGARSS.1997.608993

Awaka, J., Iguchi, T., & Okamoto, K. (2007). Rain type classification algorithm. *Measuring precipitation from space: EURAINSAT and the future* (pp. 213–224). Dordrecht: Springer.

Bacmeister, J. T., Wehner, M. F., Neale, R. B., Gettelman, A., Hannay, C., Lauritzen, P. H., et al. (2014). Exploratory high-resolution climate simulations using the Community Atmosphere Model (CAM). *Journal of Climate*, *27*(9), 3073–3099. https://doi.org/10.1175/JCLI-D-13-00387.1

Benedict, J. J., Medeiros, B., Clement, A. C., & Pendergrass, A. G. (2017). Sensitivities of the hydrologic cycle to model physics, grid resolution, and ocean type in the aquaplanet Community Atmosphere Model. *Journal of Advances in Modeling Earth Systems*, *9*, 1307–1324. https://doi.org/10.1002/2016MS000891

Biasutti, M., & Yuter, S. E. (2013). Observed frequency and intensity of tropical precipitation from instantaneous estimates. *Journal of Geophysical Research: Atmospheres*, *118*, 9534–9551. https://doi.org/10.1002/jgrd.50694

Bretherton, C. S., & Park, S. (2009). A new moist turbulence parameterization in the community atmosphere model. *Journal of Climate*, *22*(12), 3422–3448. https://doi.org/10.1175/2008JCLI2556.1

Chen, D., & Dai, A. (2018). Dependence of estimated precipitation frequency and intensity on data resolution. *Climate Dynamics*, *50*(9-10), 3625–3647. https://doi.org/10.1007/s00382-017-3830-7

Collins, W. D., Rasch, P J., Boville, B A., Hack, J. J., McCaa, J. R., Williamson, D. L., et al. (2004). Description of the NCAR community atmosphere model (CAM 3.0). Tech. Rep. NCAR/TN-464 + STR, National Center for Atmospheric Research, Boulder, CO, 226 pp.

Dai, A. (2001). Global precipitation and thunderstorm frequencies. Part I: Seasonal and interannual variations. *Journal of Climate*, *14*, 1092–1111. https://doi.org/10.1175/1520-0442(2001)014<1092:GPATFP>2.0.CO;2

Dai, A. (2006). Precipitation characteristics in eighteen coupled climate models. *Journal of Climate*, *19*(18), 4605–4630. https://doi.org/10.1175/JCLI3884.1

Dai, A., Giorgi, F., & Trenberth, K. E. (1999). Observed and model simulated diurnal cycles of precipitation over the contiguous United States. *Journal of Geophysical Research*, *104*(D6), 6377–6402. https://doi.org/10.1029/98JD02720

Dai, A., Lin, X., & Hsu, K. (2007). The frequency, intensity, and diurnal cycle of precipitation in surface and satellite observations over low- and mid-latitudes. *Climate Dynamics*, *29*(7-8), 727–744. https://doi.org/10.1007/s00382-007-0260-y

Dai, A., Rasmussen, R. M., Liu, C., Ikeda, I., & Prein, A. F. (2017). A new mechanism for warm-season precipitation response to global warming based on convection-permitting simulations. *Climate Dynamics*. https://doi.org/10.1007/s00382-017-3787-6

Dai, A., & Trenberth, K. E. (2004). The diurnal cycle and its depiction in the community climate system model. *Journal of Climate*, *117*, 930–951. https://doi.org/10.1175/1520-0442(2004)017<0930:TDCAID>2.0.CO;2

DeMott, C. A., Randall, D. A., & Khairoutdinov, M. (2007). Convective precipitation variability as a tool for general circulation model analysis. *Journal of Climate*, *20*(1), 91–112. https://doi.org/10.1175/JCLI3991.1

Dwyer, J. G., & O'Gorman, P. A. (2017). Changing duration and spatial extent of midlatitude precipitation extremes across different climates. *Geophysical Research Letters*, *44*, 5863–5871. https://doi.org/10.1002/2017GL072855

Flato, G., Marotzke, J., Abiodun, B., Braconnot, P., Chou, S. C., Collins, W., et al. (2013). Evaluation of climate models. In T. F. Stocker, D. Qin, G.-K. Plattner, M. Tignor, S. K. Allen, J. Boschung, et al. (Eds.), *Climate Change 2013: The Physical Science Basis. Contribution of Working Group I to the Fifth Assessment Report of the Intergovernmental Panel on Climate Change* (pp. 741–866). Cambridge, United Kingdom and New York, NY, USA: Cambridge University Press.

Gehne, M., Hamill, T. M., Kiladis, G. N., & Trenberth, K. E. (2016). Comparison of global precipitation estimates across a range of temporal and spatial scales. *Journal of Climate*, *29*(21), 7773–7795. https://doi.org/10.1175/JCLI-D-15-0618.1

Gettelman, A., Morrison, H., & Ghan, S. J. (2008). A new two-moment bulk stratiform cloud microphysics scheme in the NCAR Community Atmosphere Model (CAM3. Part II: Single-column and global results). *Journal of Climate*, *21*(15), 3660–3679. https://doi.org/10.1175/2008JCLI2116.1

Gustafson, W. I., Ma, P.-L., & Singh, B. (2014). Precipitation characteristics of CAM5 physics at mesoscale resolution during MC3E and the impact of convective timescale choice. *Journal of Advances in Modeling Earth Systems*, *6*, 1271–1287. https://doi.org/10.1002/2014MS000334

Hack, J. J. (1994). Parameterization of moist convection in the national center for atmospheric research Community Climate Model (CCM2). *Journal of Geophysical Research*, *99*(D3), 5551–5568. https://doi.org/10.1029/93JD03478

Held, I. M., Zhao, M., & Wyman, B. (2007). Dynamic radiative–convective equilibria using GCM column physics. *Journal of the Atmospheric Sciences*, *64*(1), 228–238. https://doi.org/10.1175/JAS3825.11

Herold, N., Alexander, L. V., Donat, M. G., Contractor, S., & Becker, A. (2016). How much does it rain over land? *Geophysical Research Letters*, *43*, 341–348. https://doi.org/10.1002/2015GL066615

Holtslag, A., & Boville, B. (1993). Local versus nonlocal boundary-layer diffusion in a global climate model. *Journal of Climate*, *6*(10), 1825–1842. https://doi.org/10.1175/1520-0442(1993)006<1825:LVNBLD>2.0.CO;2

Houze, R. A. (2004). Mesoscale convective systems. *Reviews of Geophysics*, *42*, RG4003. https://doi.org/10.1029/2004RG000150

Houze, R. A., Rasmussen, K. L., Zuluaga, M. D., & Brodzik, S. R. (2015). The variable nature of convection in the tropics and subtropics: A legacy of 16 years of the Tropical Rainfall Measuring Mission satellite. *Reviews of Geophysics*, *53*, 994–1021. https://doi.org/10.1002/2015RG000488

Huffman, G. J., Adler, R. F., Bolvin, D. T., & Gu, G. (2009). Improving the global precipitation record: GPCP version 2.1. *Geophysical Research Letters*, *36*, L17808. https://doi.org/10.1029/2009GL040000

Huffman, G. J., Adler, R. F., Bolvin, D. T., Wolff, D. B., Gu, G., Nelkin, E. J., et al. (2007). The TRMM multisatellite precipitation analysis (TMPA): Quasi-global, multiyear, combined-sensor precipitation estimates at fine scales. *Journal of Hydrometeorology*, *8*(1), 38–55. https://doi.org/10.1175/JHM560.1

Hurrell, J. W., Holland, M. M., Gent, P. R., Ghan, S., Kay, J. E., Kushner, P. J., et al. (2013). The Community Earth System Model. *Bulletin of the American Meteorological Society*, *94*(9), 1339–1360. https://doi.org/10.1175/BAMS-D-12-00121.1

Kay, J. E., L'Ecuyer, T., Pendergrass, A., Chepfer, H., Guzman, R., & Yettella, V. (2018). Scale-aware and definition-aware evaluation of modeled near-surface precipitation frequency using CloudSat observations. *Journal of Geophysical Research: Atmospheres*, *123*, 4294–4309. https://doi.org/10.1002/2017JD028213

Kendon, E., Ban, N., Roberts, N., Fowler, H., Roberts, M., Chan, S., et al. (2016). Do convection-permitting regional climate models improve projections of future precipitation change? *Bulletin of the American Meteorological Society*, *98*(1), 79–93. https://doi.org/10.1175/BAMS-D-15-0004.1

Kooperman, G. J., Pritchard, M. S., Burt, M. A., Branson, M. D., & Randall, D. A. (2016). Robust effects of cloud superparameterization on simulated daily rainfall intensity statistics across multiple versions of the Community Earth System Model. *Journal of Advances in Modeling Earth Systems*, *8*, 140–165. https://doi.org/10.1002/2015MS000574

Kooperman, G. J., Pritchard, M. S., O'Brien, T. A., & Timmermans, B. W. (2018). Rainfall from resolved rat her than parameterized processes better represents the present-day and climate change response of moderate rates in the community atmosphere model. *Journal of Advances in Modeling Earth Systems*, *10*, 971–988. https://doi.org/10.1002/2017MS001188

Kopparla, P., Fischer, E. M., Hannay, C., & Knutti, R. (2013). Improved simulation of extreme precipitation in a high-resolution atmosphere model. *Geophysical Research Letters*, *40*, 5803–5808. https://doi.org/10.1002/2013GL057866

Lau, W. K. M., Wu, H. T., & Kim, K. M. (2013). A canonical response of precipitation characteristics to global warming from CMIP5 models. *Geophysical Research Letters*, *40*, 3163–3169. https://doi.org/10.1002/grl.50420

Li, F., Collins, W. D., Wehner, M. F., Williamson, D., Olson, J., & Algieri, C. (2011). Impact of horizontal resolution on simulation of precipitation extremes in an aqua-planet version of Community Atmospheric Model (CAM3). *Tellus*, *63*(5), 884–892. https://doi.org/10.1111/j.1600-0870.2011.00544.x

Ma, P.-L., Rasch, P. J., Fast, J. D. R., Easter, C., Gustafson, W. I. Jr., Liu, X., et al. (2014). Assessing the CAM5 physics suite in the WRF-Chem model: implementation, resolution sensitivity, and a first evaluation for a regional case study. *Geoscientific Model Development*, *7*(3), 755–778. https://doi.org/10.5194/gmd-7-755-2014

Morrison, H., & Gettelman, A. (2008). A new two-moment bulk stratiform cloud microphysics scheme in the Community Atmosphere Model version 3 (CAM3). Part I: Description and numerical tests. *Journal of Climate*, *21*(15), 3642–3659. https://doi.org/10.1175/2008JCLI2105.1

Morrison, H., Thompson, G., & Tatarskii, V. (2009). Impact of cloud microphysics on the development of trailing stratiform precipitation in a simulated squall line: Comparison of one-and two-moment schemes. *Monthly Weather Review*, *137*(3), 991–1007. https://doi.org/10.1175/2008MWR2556.1

Neale, R. B., Gettelman, A., Park, S., Conley, A. J., Kinnison, D., Marsh, D., et al. (2012). Description of the NCAR Community Atmosphere Model (CAM 5.0). Tech. Rep. NCAR/TN-486 + STR, National Center for Atmospheric Research, Boulder, Colo.

Neale, R. B., Richter, J. H, Conley, A. J., Park, S., Lauritzen, P. H., Gettelan, A., et al. (2010). Description of the NCAR Community Atmosphere Model (CAM 4.0). Tech. Rep. NCAR/TN-485 + STR, National Center for Atmospheric Research, Boulder, Colo.

Nikolopoulos, E. I., Destro, E., Maggioni, V., Marra, F., & Borga, M. (2017). Satellite rainfall estimates for debris flow prediction: an evaluation based on rainfall accumulation–duration thresholds. *Journal of Hydrometeorology*, *18*(8), 2207–2214. https://doi.org/10.1175/JHM-D-17-0052.1

O'Brien, T. A., Collins, W. D., Kashinath, K., Rubel, O., Byna, S., Gu, J., et al. (2016). Resolution dependence of precipitation statistical fidelity in hindcast simulations. *Journal of Advances in Modeling Earth Systems*, *8*, 976–990. https://doi.org/10.1002/2016MS000671

O'Brien, T. A., Li, F., Collins, W. D., Rauscher, S. A., Ringler, T. D., Taylor, M. S., et al. (2013). Observed scaling in clouds and precipitation and scale incognizance in regional to global atmospheric models. *Journal of Climate*, *26*(23), 9313–9333. https://doi.org/10.1175/JCLI-D-13-00005.1

Park, S., & Bretherton, C. S. (2009). The University of Washington shallow convection and moist turbulence schemes and their impact on climate simulations with the Community Atmosphere Model. *Journal of Climate*, *22*(12), 3449–3469. https://doi.org/10.1175/2008JCLI2557.1

Pendergrass, A. G., & Deser, C. (2017). Climatological characteristics of typical daily precipitation. *Journal of Climate*, *30*(15), 5985–6003. https://doi.org/10.1175/JCLI-D-16-0684.1

Pendergrass, A. G., & Hartmann, D. L. (2014a). Changes in the distribution of rain frequency and intensity in response to global warming. *Journal of Climate*, *27*(22), 8372–8383. https://doi.org/10.1175/JCLI-D-14-00183.1

Pendergrass, A. G., & Hartmann, D. L. (2014b). The atmospheric energy constraint on global–mean precipitation change. *Journal of Climate*, *27*(2), 757–768. https://doi.org/10.1175/JCLI-D-13-00163.1

Prein, A. F., Langhans, W., Fosser, G., Ferrone, A., Ban, N., Goergen, K., et al. (2015). A review on regional convection-permitting climate modeling: Demonstrations, prospects, and challenges. *Reviews of Geophysics*, *53*, 323–361. https://doi.org/10.1002/2014RG000475

Qian, T., Dai, A., Trenberth, K. E., & Oleson, K. W. (2006). Simulation of global land surface conditions from 1948–2004. Part I: Forcing data and evaluation. *Journal of Hydrometeorology*, *7*(5), 953–975. https://doi.org/10.1175/JHM540.1

Rasch, P., & Kristjánsson, J. (1998). A comparison of the CCM3 model climate using diagnosed and predicted condensate parameterizations. *Journal of Climate*, *11*(7), 1587–1614. https://doi.org/10.1175/1520-0442(1998)011<1587:ACOTCM>2.0.CO;2

Rasch, P. J., Stevens, M. J., Ricciardulli, L., Dai, A., Negri, A., Wood, R., et al. (2006). A characterization of tropical transient activity in the CAM3 atmospheric hydrologic cycle. *Journal of Climate*, *19*(11), 2222–2242. https://doi.org/10.1175/JCLI3752.1

Rauscher, S. A., O'Brien, T. A., Piani, C., Coppola, E., Giorgi, F., Collins, W. D., & Lawston, P. M. (2016). A multimodel intercomparison of resolution effects on precipitation: Simulations and theory. *Climate Dynamics*, *47*(7-8), 2205–2218. https://doi.org/10.1007/s00382-015-2959-5

Sakaguchi, K., Leung, L. R., Burleyson, C. D., Xiao, H., & Wan, H. (2018). Role of troposphere-convection-land coupling in the southwestern Amazon precipitation bias of the community Earth system model version 1 (CESM1). *Journal of Geophysical Research: Atmospheres*, *123*, 8374–8399. https://doi.org/10.1029/2018JD028999

Schumacher, C., & Houze, R. A. Jr. (2003). Stratiform rain in the tropics as seen by the TRMM precipitation radar. *Journal of Climate*, *16*(11), 1739–1756. https://doi.org/10.1175/1520-0442(2003)016<1739:SRITTA>2.0.CO;2

Trenberth, K. E. (2011). Changes in precipitation with climate change. *Climate Research*, *47*(1), 123–138. https://doi.org/10.3354/cr00953

Trenberth, K. E., Dai, A., Rasmussen, R. M., & Parsons, D. B. (2003). The changing character of precipitation. *Bulletin of the American Meteorological Society*, *84*(9), 1205–1218. https://doi.org/10.1175/BAMS-84-9-1205

Trenberth, K. E., & Zhang, Y. (2018a). How often does it really rain? *Bulletin of the American Meteorological Society*, *99*(2), 289–298. https://doi.org/10.1175/BAMS-D-17-0107.1

Trenberth, K. E., & Zhang, Y. (2018b). Near-global covariability of hourly precipitation in space and time. *Journal of Hydrometeorology*, *19*(4), 695–713. https://doi.org/10.1175/JHM-D-17-0238.1

Trenberth, K. E., Zhang, Y. X., & Gehne, M. (2017). Intermittency in precipitation: duration, frequency, intensity, and amounts using hourly data. *Journal of Hydrometeorology*, *18*(5), 1393–1412. https://doi.org/10.1175/JHM-D-16-0263.1

Tropical Rainfall Measuring Mission (TRMM) (2011a). TRMM radar rainfall statistics L3 1 month (5 × 5) and (0.5 × 0.5) degree V7, Greenbelt, MD, Goddard Earth Sciences Data and Information Services Center (GES DISC). Accessed: [2017-12-01], https://disc.gsfc.nasa.gov/datacollection/TRMM_3A25_7.html

Tropical Rainfall Measuring Mission (TRMM) (2011b). TRMM (TMPA) Rainfall estimate L3 3 hour 0.25 degree x 0.25 degree V7, Greenbelt, MD, Goddard Earth Sciences Data and Information Services Center (GES DISC). Accessed: [2017-01-01], https://doi.org/10.5067/TRMM/TMPA/3H/7

Wehner, M. F., Reed, K. A., Li, F., Prabhat, Bacmeister, J., Chen, C. T., et al. (2014). The effect of horizontal resolution on simulation quality in the Community Atmosphere Model, CAM5.1. *Journal of Advances in Modeling Earth Systems*, *6*, 980–997. https://doi.org/10.1002/2013MS000276

Wilcox, E. M., & Donner, L. J. (2007). The frequency of extreme rain events in satellite rain-rate estimates and an atmospheric general circulation model. *Journal of Climate*, *20*(1), 53–69. https://doi.org/10.1175/JCLI3987.1

Williamson, D. L. (2013). The effect of time steps and time-scales on parametrization suites. *Quarterly Journal of the Royal Meteorological Society*, *139*(671), 548–560. https://doi.org/10.1002/qj.1992

Xie, S. C., Zhang, M. H., Boyle, J. S., Cederwall, R. T., Potter, G. L., & Lin, W. Y. (2004). Impact of a revised convective triggering mechanism on Community Atmosphere Model, version 2, simulations: Results from short-range weather forecasts. *Journal of Geophysical Research*, *109*, D14102. https://doi.org/10.1029/2004JD004692

Yang, B., Qian, Y., Lin, G., Leung, L. R., Rasch, P. J., Zhang, G. J., et al. (2013). Uncertainty quantification and parameter tuning in the CAM5 Zhang-McFarlane convection scheme and impact of improved convection on the global circulation and climate. *Journal of Geophysical Research: Atmospheres*, *118*, 395–415. https://doi.org/10.1029/2012JD018213

Yang, S., & Smith, E. A. (2008). Convective–stratiform precipitation variability at seasonal scale from 8 yr of TRMM observations: Implications for multiple modes of diurnal variability. *Journal of Climate*, *21*(16), 4087–4114. https://doi.org/10.1175/2008JCLI2096.1

Zarzycki, C. M., Levy, M. N., Jablonowski, C., Overfelt, J. R., Taylor, M. A., & Ullrich, P. A. (2014). Aquaplanet experiments using CAM's variable resolution dynamical core. *Journal of Climate*, *27*(14), 5481–5503. https://doi.org/10.1175/JCLI-D-14-00004.1

Zhang, G. J., & McFarlane, N. A. (1995). Sensitivity of climate simulations to the parameterization of cumulus convection in the Canadian climate centre general circulation model. *Atmosphere-Ocean*, *33*(3), 407–446. https://doi.org/10.1080/07055900.1995.9649539

Zhang, M., Lin, W., Bretherton, C. B., Hack, J. J., & Rasch, P. J. (2003). A modified formulation of fractional stratiform condensation rate in the NCAR Community Atmosphere Model (CAM2). *Journal of Geophysical Research*, *108*(D1), 4035. https://doi.org/10.1029/2002JD002523

Zhou, T. J., Yu, R. C., Chen, H. M., Dai, A., & Pan, Y. (2008). Summer precipitation frequency, intensity, and diurnal cycle over China: A comparison of satellite data with rain gauge observations. *Journal of Climate*, *21*(16), 3997–4010. https://doi.org/10.1175/2008JCLI2028.1